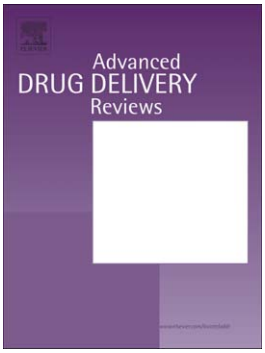

Overcoming ocular drug delivery barriers through the use of pHysical forces

Di Huang, Ying-Shan Chen, Ilva D. Rupenthal

PII: S0169-409X(17)30189-8
DOI: doi:10.1016/j.addr.2017.09.008
Reference: ADR 13178

To appear in: *Advanced Drug Delivery Reviews*

Received date: 23 November 2016
Revised date: 30 June 2017
Accepted date: 8 September 2017

Please cite this article as: Di Huang, Ying-Shan Chen, Ilva D. Rupenthal, Overcoming ocular drug delivery barriers through the use of pHysical forces, *Advanced Drug Delivery Reviews* (2017), doi:10.1016/j.addr.2017.09.008

Overcoming ocular drug delivery barriers through the use of physical forces

Di Huang, Ying-Shan Chen, Ilva D. Rupenthal*

Buchanan Ocular Therapeutics Unit, Department of Ophthalmology, New Zealand National Eye Centre, Faculty of Medical and Health Sciences, The University of Auckland, Private Bag 92019, Auckland 1142, New Zealand

*Corresponding author: Tel.: +64 9 9236386; Fax: +64 9 3677173. E-mail address: i.rupenthal@auckland.ac.nz (I.D. Rupenthal).

Abstract

Overcoming the physiological barriers in the eye remains a key obstacle in the field of ocular drug delivery. While ocular barriers naturally have a protective function, they also limit drug entry into the eye. Various pharmaceutical strategies, such as novel formulations and physical force-based techniques, have been investigated to weaken these barriers and transport therapeutic agents effectively to both the anterior and the posterior segments of the eye. This review summarizes and discusses the recent research progress in the field of ocular drug delivery with a focus on the application of physical methods, including electrical fields, sonophoresis, and microneedles, which can enhance penetration efficiency by transiently disrupting the ocular barriers in a minimally or non-invasive manner.

Keywords

Ocular drug delivery; Physiological barriers; Electrical fields; Iontophoresis; Electroporation; Sonophoresis; Microneedles

Graphical abstract

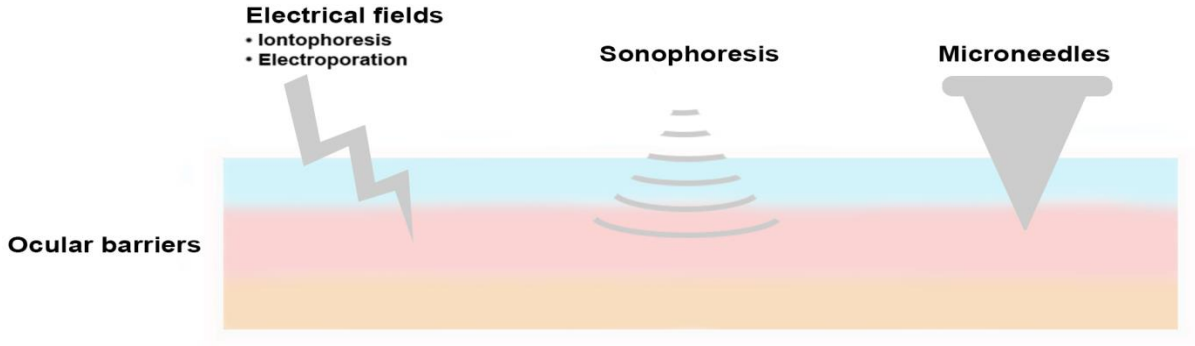

Abbreviations

AMD, age-related macular degeneration; BAB, blood-aqueous barrier; BC, Bruch's-choroid; Bev, bevacizumab; BRB, blood-retinal barrier; BSA, bovine serum albumin; Dex, dexamethasone; DSP, dexamethasone sodium phosphate; DMPC, dimyristoyl-phosphatidylcholine; DPPC, dipalmitoyl-phosphatidyl-choline; ECM, extracellular matrix; GAPDH, glyceraldehyde-3-phosphate dehydrogenase; HIFU, high intensity focused ultrasound; IgG, Immunoglobulin G; ILM, inner limiting membrane; IOP, intraocular pressure; MBs, microbubbles; MNP, microneedle pen; MNs, microneedles; MW, molecular weight; ODNs; oligodeoxynucleotides; PAMAM, polyamidoamine; PDMS, poly(dimethylsiloxane); PEDOT, poly(3,4-ethylenedioxythiophene); PLA, poly(D, L-lactide); POPC, palitoyl-oleyl-phosphatidylcholine; PRF, pulse repetition frequency; PSS, polystyrene sulfonic acid; PVP, polyvinylpyrrolidone; RCE, retinal capillary endothelium; RPE, retinal pigment epithelium; SCS, suprachoroidal space; S-ODNs, phosphorothioate oligodeoxynucleotides; ssDNA, single stranded DNA; US, ultrasound; TA, triamcinolone acetonide; β-PDE, phosphodiesterase β-subunit.

Contents

1. Introduction

Numerous people worldwide suffer from ocular diseases and many of these, including age-related macular degeneration (AMD), diabetic retinopathy, cataract, uveitis, and glaucoma, directly affect the patient's vision and thus the quality of life. The estimated number of people visually impaired in the world is 285 million, with 39 million blind and 246 million suffering from low vision [1]. As these numbers will continue to rise due to the world population growth, vision impairment and blindness are becoming ubiquitous causes of disability [2]. Over the past decades, a number of novel therapies have been developed to halt or even treat some of these conditions; however, efficient ocular delivery of macromolecules and gene therapeutics still remains a challenge.

Delivering therapeutic agents to specific intraocular targets and achieving an optimal drug concentration is limited by a number of inherent anatomical and physiological ocular barriers, including the cornea and anterior segment barriers, the sclera and Bruch's-choroid complex as well as the blood-retinal barrier (BRB). The presence of these natural barriers not only protects the eye from invasion of foreign substances but also regulates the milieu of the intraocular tissues, which is essential for maintaining the ocular physiological function [3]. However, these tight barriers also pose major obstacles for efficient drug delivery as they limit the diffusion and penetration of ophthalmic agents. Overcoming these barriers and improving ocular drug bioavailability is thus a challenging task. Various pharmaceutical strategies aimed at weakening these physiological barriers and thus enhancing the permeability of ocular drugs have been investigated over recent decades. These strategies can generally be divided into formulation- and physical force-based techniques. Formulation-based approaches utilize chemical penetration enhancers [4], prodrugs [5], penetrating peptides [6], and drug delivery carriers such as liposomes [7] and nano- or microparticles [8] to increase drug penetration across these barriers. Physical force-based methods, on the other hand, generally require a physical device, driven by a power generator, to deliver energy to the barriers resulting in transient drug transport enhancement or to physically breach these barriers. Compared to formulation-based approaches, physical force-based strategies can better control the drug dose while also being able to record parameter information. However, when used to target accessible ocular tissues such as the cornea and the sclera, a custom designed device is generally required which can be expensive, as ocular tissues are unique and sensitive, with the external energy source potentially causing damage to the eye.

Various devices based on physical forces such as electrical fields [9], sonophoresis [10], and microneedles [11], have been developed to enhance ocular drug delivery by temporarily disrupting the barrier structures. While the use of physical methods has been intensively investigated for transdermal delivery [12], there are only limited ocular drug delivery reports, although a number of studies have

demonstrated that small molecules, macromolecules, genetic materials, and even drug delivery carriers such as nanoparticles and dendrimers can be successfully delivered into the eye by physical forces without detectable ocular tissue damage. This review summarizes and discusses recent advances in ocular drug delivery using physical methods.

2. Physiological barriers to efficient ocular drug delivery

Drugs can be delivered into the eye via anterior or posterior segment routes depending on the target site. Each layer of the ocular tissues has special characteristics and poses a different barrier following drug administration via a certain route (**Fig. 1**).

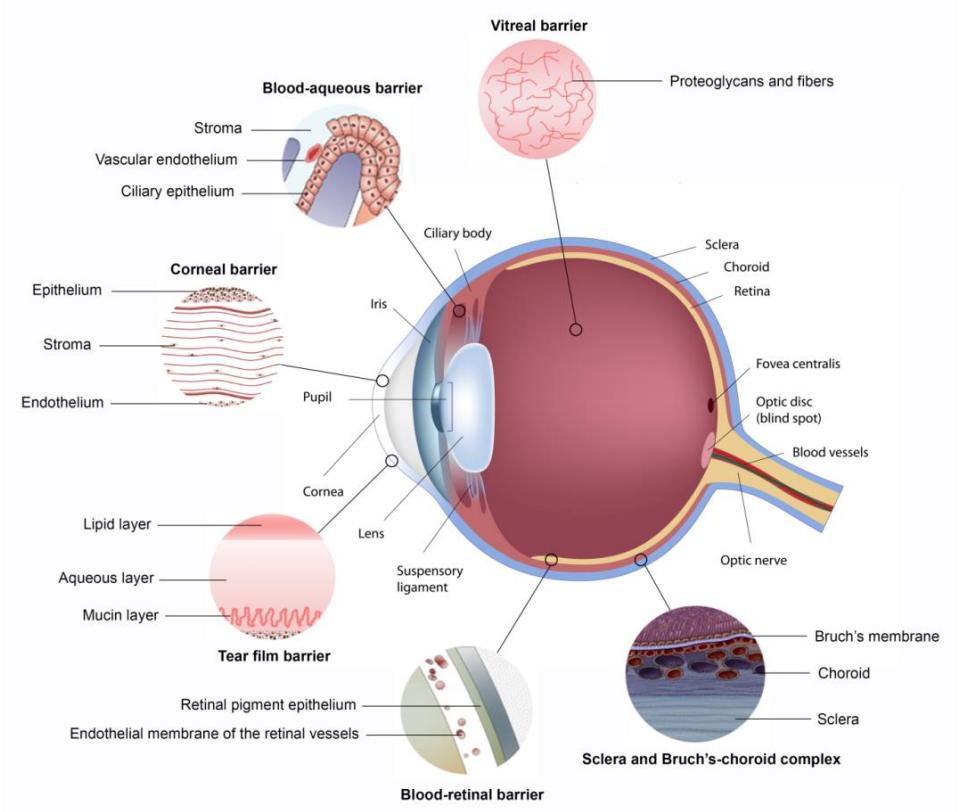

Fig. 1. Physiological barriers in ocular drug delivery.

2.1. Cornea and anterior segment barriers

The cornea is a 0.5 mm thick transparent collagenous structure and the primary barrier to topical drug absorption [13]. Physiologically, the cornea consists of five recognized layers, three cellular layers (epithelium, stroma, and endothelium) and two interface layers (Bowman's and Descemet's membrane). The most critical barrier to penetration is the epithelium, which consists of six to eight layers of cells and strictly controls the permeability of solutes. Epithelial cells become flatter during

maturation and eventually form tight intercellular junctions with a tiny paracellular pore diameter of 2.0 nm resulting in a relatively tight diffusion barrier for drug absorption from the tear fluid to the anterior chamber. Thus only molecules with a molecular radius of less than 5.5 Å or a molecular weight (MW) of 500 Da are generally able to penetrate across the corneal epithelium through the paracellular route [14, 15]. As such, drug passage across the cornea mainly depends on the physicochemical characteristics of the molecule, with epithelium and endothelium preventing hydrophilic molecules to pass into the aqueous humor, while permitting the passage of small lipophilic molecules. The stroma, on the other hand, resists the passage of lipophilic molecules but allows diffusion of hydrophilic drugs. This sandwich-like structure makes the cornea a unique barrier to most lipophilic and hydrophilic drugs. Thus, only small molecules possessing the optimal lipophilicity (log *D* values between 2 to 3) can efficiently penetrate these layers [16]. In addition to the MW and the lipophilicity of the molecule, corneal permeability is also heavily affected by the charge of the solute. The corneal surface is generally negatively charged above its isoelectric point of 3.2. Consequently, cationic compounds bind to and permeate more easily across the cornea than anionic species [17]. Below its isoelectric point, the cornea is more permeable to anionic molecules [18]; however, applying highly acidic formulations to achieve a tissue pH of 3.2 is impractical in the clinical setting due to the strong tissue irritation. Overall, the charge discriminating effect of the cornea primarily decreases the absorption of negatively charged molecules. Besides the corneal barrier itself, there is also a constant flow of tear fluid across the outer surface of the eye with 50% of the normal human tear film being replaced every 2 to 20 min [19]. This significantly reduces drug residence on the ocular surface thus decreasing the time for absorption with most eye drops being completely washed away within minutes. All of these factors limit drug penetration into or across the cornea resulting in low drug bioavailability of generally less than 5% for most topically applied drugs with this value even lower for macromolecules [20].

The conjunctiva is a thin translucent vascularized mucus membrane, which can be divided into three portions, including the bulbar conjunctiva, conjunctival fornix as well as the palpebral conjunctiva [21]. It is composed of two layers: an outer epithelium that acts as the major penetration barrier and its underlying stroma. In humans, the conjunctiva occupies a 17-fold larger surface area than the cornea [22] generally allowing for higher absorption to occur across this tissue. Also, intercellular spacing in the conjunctival epithelium is wider than that in the corneal epithelium, being 3.0 nm in the bulbar and 4.9 nm in the palpebral conjunctiva [23], thus the permeability of drugs across the conjunctiva is generally greater than across the cornea. For example, the conjunctival permeability of hydrophilic mannitol was found to be about 55-fold higher than its corneal permeability while the conjunctiva was also permeable to molecules with higher MWs (up to 10 kDa) [24]. However, drug absorption through the conjunctiva is still minimal due to the presence of conjunctival blood capillaries and lymphatics,

which can cause significant drug loss into the systemic circulation thereby lowering the overall ocular bioavailability.

The intraocular environment, such as the aqueous humor, is also protected by the blood-aqueous barrier (BAB). Two discrete cellular layers (the endothelium of the iris-ciliary blood vessels and the non-pigmented ciliary epithelium) form the BAB in the anterior segment of the eye, which controls the traverse of solutes between the anterior and posterior segment and is poorly permeable due to the presence of tight junctions. It is generally considered impractical to treat anterior segment disorders by intravenous injection, as the BAB prevents the passage of plasma-derived albumin and hydrophilic drugs from the plasma into the aqueous humor. This is strongly impacted by the MW of the solute; thus, concentrations of solutes in the aqueous humor generally decrease with increasing MW, suggesting the presence of a selective barrier or molecular sieve [25]. Furthermore, the passage of drugs from the anterior to the posterior segment is limited by the BAB because of the continuous drainage of aqueous humor with a turnover rate of 2.0 to 3.0 mL/min [26]. Therefore, conventional topical eye drop administration generally fails to provide efficient drug concentrations for the treatment of posterior segment diseases.

2.2. Sclera and Bruch's-choroid complex

The human sclera has a large and accessible surface area of approximately 16.3 cm^2 and mainly consists of an extracellular matrix consisting of collagen fibrils and glycoproteins [27]. It is generally more permeable to solutes than the cornea and the conjunctiva, especially to hydrophilic compounds, as transscleral diffusion is primarily a matter of diffusion through an aqueous medium of proteoglycans or porous spaces within the collagen network (25 to 300 nm in diameter) rather than diffusion across cellular membranes [28, 29]. Similar to other ocular tissues, scleral permeability is strongly dependent on the drug MW, with macromolecules exhibiting lower permeability than small molecules [30]. However, for the sclera the molecular radius seems to be a better predictor of macromolecule (e.g. dextrans and proteins) permeability than the MW. For example, the scleral permeability of a 70 kDa dextran was not significantly greater than for a 150 kDa dextran, whereas a globular protein with a molecular radius of 5.23 nm was more permeable than a linear dextran of the same MW, but with a molecular radius of 8.25 nm [31]. Transscleral permeability is also strongly influenced by the charge of the molecule. Opposite to the permeation across the cornea, positively charged molecules have lower permeability across the sclera than those with negative charges, as the proteoglycan matrix of the sclera is negatively charged, which contributes to the binding of positively charged solutes and hinders their transport across the tissue [32]. Nevertheless, recent literature has highlighted the difficulties in predicting macromolecular behavior based on physicochemical properties due to interactions between molecular radius, charge, and molecular conformation thus preventing individual analysis of these factors [33].

The choroid is a significant dynamic barrier, as it is a highly vascularized and innervated tissue supplying blood to the retina. It is composed of a network of fenestrated capillaries and supported by Bruch's membrane, which is a thin (2 to 4 μm), pentalamellar, elastic membrane that also represents the basement membrane of the retinal pigment epithelium (RPE). Bruch's-choroid (BC) complex poses a more critical barrier to drug delivery by the transscleral route than the sclera itself, as it is more discriminating, particularly to positively charged lipophilic drugs, due to the binding of the solute to the tissue thereby forming a slow-release drug depot in the BC complex [34-36]. Furthermore, the molecular size also affects BC complex permeability with hydrophilic carboxyfluorescein and dextrans having shown an exponential decrease with increasing molecular radius in bovine tissues [53].

2.3. Retina and blood-retinal barrier

The retina is a thin transparent tissue which forms the innermost layer of the eye and adheres to the choroid. It consists of the outer RPE and the inner neural retina. The RPE is a monolayer of polarized cells while the neural retina is composed of nine layers with the inner limiting membrane (ILM), mainly comprised of extracellular matrix (ECM) proteins, posing the most significant barrier to drug penetration [37]. The retina is considered a significant barrier to ocular drug delivery with larger molecules penetrating the retina with progressively more difficulty [38, 39]. For example, carboxyfluorescein, a small molecule with a molecular radius of 5.5 Å, could freely cross the retina from the subretinal space to the vitreous within 2 h, whereas 70 kDa (58 Å) and 150 kDa (85 Å) dextrans only penetrated the retina after 72 h [40].

The BRB mainly hinders substance diffusion from the systemic circulation into the retina [41]. It is divided into the inner and outer BRB. The inner BRB is composed of retinal capillary endothelial (RCE) cells which possess intercellular tight junctions and selectively protect the retina from foreign substances in the blood circulation, especially hydrophilic compounds and macromolecules [42-44]. The outer BRB is comprised of the RPE, which is located between the photoreceptors and the choriocapillaries [45]. The unique transport processes within the RPE along with its critical barrier characteristics strictly govern the diffusion of compounds. The molecular radius is again the major factor affecting drug diffusion across the RPE with the permeability declining exponentially with an increasing radius. For example, the permeability of 376 Da (5 Å) carboxyfluorescein was found to be 35-fold higher than that of 80 kDa (64 Å) dextran [46]. Solute lipophilicity also has an impact on the permeation across the RPE. Hydrophilic compounds permeate mainly through tight junctions (paracellular route), while lipophilic drugs cross the RPE via the transcellular route [46]. Thus, only small lipophilic molecules can transfer efficiently between choroid and retina, which limits drug delivery both in the inward (blood to vitreous) and outward (vitreous to blood) direction. **Table 1** summarizes the effect of physicochemical drug characteristics on ocular tissue permeability.

Table 1. Summary of physicochemical properties affecting ocular tissue permeability.

Ocular tissue	Molecular size	Lipophilicity	Charge
Cornea	Decreases with increasing molecular radius [15]	Preference for lipophilic molecules (log *D* 2 to 3) [16]	Preference for positively charged molecules [17]
Conjunctiva	Decreases with increasing molecular radius [23]	Preference for lipophilic molecules [47]	Not studied
BAB	Decreases with increasing MW [25, 48]	Preference for lipophilic molecules [49]	Not studied
Sclera	Decreases with increasing molecular radius [31]	Preference for hydrophilic molecules [28]	Preference for negatively charged molecules [32, 50]
BC complex	Decreases with increasing MW [51]	Preference for hydrophilic molecules [35]	Preference for negatively charged molecules [35]
BRB	Decreases with increasing molecular radius [46, 52]	Preference for lipophilic molecules [44]	Not studied

3. Enhanced ocular drug delivery using electrical fields

3.1. Iontophoresis

Iontophoresis is a technique that enhances drug delivery across biological membranes by application of a low-intensity electrical current [53]. Due to its recognizable advantages, such as ease of application, minimal or non-invasiveness, and increased drug penetration directly into the target tissue, iontophoresis has been intensively investigated for drug delivery across various barriers, including the skin [54], nails [55], and eyes [56]. Ocular iontophoresis was first reported by Wirtz [57], who studied iontophoresis mediated topical delivery of zinc salts in the treatment of corneal ulcers, keratitis, and episcleritis. Over recent decades, there has been an increasing number of studies using iontophoresis to deliver small molecules [58], macromolecules [59], and nanocarriers [60, 61] to the eye.

3.1.1. Underlying mechanisms of iontophoresis

The mechanism of iontophoretic drug delivery is a net effect of the permeability enhancement due to electrorepulsion and electroosmosis [62]. Electrorepulsion is the movement of ionic species in the presence of an electrical field [63], while electroosmosis can enhance the transport of both neutral and charged permeants. A convective solvent flow is hereby induced under the electrical field, which occurs when a voltage difference is imposed across a charged membrane [64].

The cornea and sclera have an isoelectric point of approximately 3.2 and 3.0, respectively [18, 65], thus they are negatively charged at physiological pH. Upon exposure to an electrical field, the negatively charged cornea and sclera are responsible for the electroosmotic flow which is generated in the direction of the counterion flow to neutralize the membrane charge, i.e. from the anode to the cathode. This streaming potential has been considered as an alternative tool to study the permselectivity of biological membranes as it can give detailed information on the biomechanical characteristics and helps in better understanding the iontophoretic mechanisms [66].

The relative contribution of electrorepulsion and electroosmosis depends upon both, the physicochemical characteristics of the permeating species (e.g. size, charge, and charge to MW ratio) and the electrical features of the biological membrane. In general, iontophoretic permeability enhancement of small charged molecules is mainly governed by electrorepulsion, along with a minor contribution of electroosmosis, while for macromolecules the mechanisms is highly dependent on the charge to MW ratio. For example, for anionic macromolecules with a low charge to mass ratio such as bovine serum albumin (BSA, MW 69 kDa) and bevacizumab (Bev, MW 149 kDa), more efficient transport was observed during anodal compared to cathodal iontophoresis, suggesting that electroosmosis was the major contributing mechanism in the iontophoretic transport of such macromolecules. Contrary, when highly negatively charged polyelectrolytes such as polystyrene sulfonic acid (PSS, MW 69 kDa), having a high charge to mass ratio, were employed, higher permeability enhancement was found with the application of cathodal compared to anodal iontophoresis, which was likely a result of the dominant effect of electrorepulsion. The difference in the iontophoretic mechanism and thus the transport enhancement of macromolecules is thus mainly governed by the charge to mass ratio of the molecule [59, 65]. Other factors affecting the principal mechanism of iontophoretic delivery include electrophoretic and relaxation effects as well as changes in the biological membrane properties caused by the transported molecules and/or the electric field during iontophoresis. For example, the rate of electroosmotic flow can be influenced by the charge of the delivered species which can interact with the biological membrane changing its charge profile and thus barrier properties [67].

3.1.2. Ocular iontophoresis devices

The basic design of ocular iontophoretic devices consists of a power source and two electrodes: the donor electrode (ocular applicator) and the return electrode. The drug is filled into the applicator and the return electrode is placed at a distal site on the body, generally on the forehead, to form an electrical circuit **(Fig. 2)** [53].

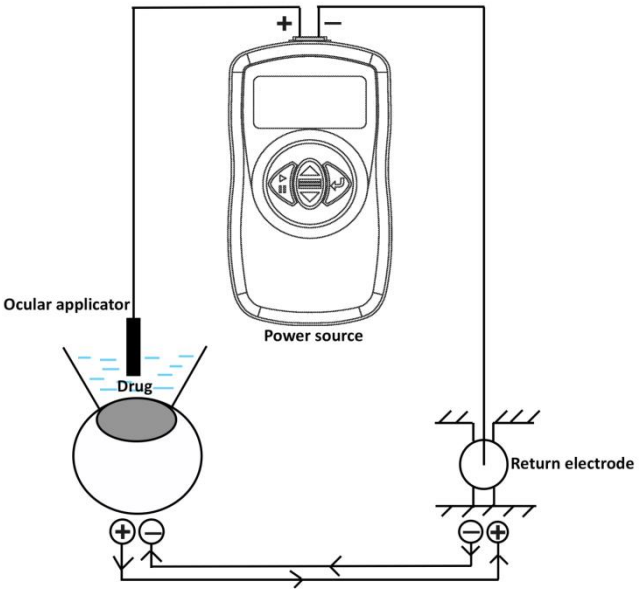

Fig. 2. Diagram of an ocular anodal iontophoresis set-up for delivery of a positively charged drug.

Eye cups, one of the most common ocular iontophoretic devices, are used to deliver drugs by filling the drug solution into the cup during the iontophoretic procedure. EyeGate®, an annular shaped silicone probe with a 0.5 cm^2 contact area and a 13 mm inner diameter for transscleral iontophoresis, was firstly designed by the Optis Group (Paris, France) and further developed into the EyeGate II Delivery System by EyeGate Pharmaceuticals Inc. (Waltham, MA, USA). This iontophoretic device is currently being investigated to treat various ocular inflammatory disorders by delivering a sustained release dexamethasone (Dex) formulation (EGP-437) and is in clinical trials for the treatment of anterior uveitis (Phase 3) [68, 69], dry eye (Phase 3) [70, 71] and macular edema (Phase 1 and 2) [72] as well as for preventing ocular inflammation in patients who have undergone cataract surgery (Phase 2) [73, 74]. A novel device using a biocompatible planar poly(3,4-ethylenedioxythiophene) (PEDOT) electrode was recently designed to enhance iontophoretic efficiency, as PEDOT electrodes have a better charge capacity and stability than commonly used metallic electrodes (e.g. platinum and silver/silver chloride). Also, PEDOT can be fabricated into an extremely small-sized applicator (4 mm inner diameter) which can be placed under the eyelid to deliver ions through a small settled portion on the eyeball thereby reducing tissue damage during ion penetration when compared to conventional eye cups [75, 76].

Another application utilizes a drug saturated hydrogel pad as the delivery probe with the loading of the drug into the hydrogel facilitating the handling and minimizing tissue hydration and current interruptions [77]. Such a portable battery operated ocular iontophoretic device was designed by an Israeli team, composed of a cylindrical well for insertion of the disposable hydrogel, two electrodes, and a panel for time and current control. Various formulations, including gentamicin [78], Dex [79],

methylprednisolone [80], as well as charged nanoparticles [81], have been loaded into the hydrogel and have been evaluated for transcorneal or transscleral iontophoresis with promising results. The OcuPhor™ Delivery System, a custom manufactured hydrogel composed of a polyacetal sponge for transscleral iontophoresis, was developed by IOMED Inc. (Salt Lake City, Utah, USA). The drug applicator (dry hydrogel pad) is infused with the formulation before application and is then placed onto the sclera. Animal studies indicated that the drug was delivered into the retina and choroid of rabbits in a targeted and controlled manner and clinical trials in healthy volunteers showed an excellent safety profile for the current range employed [82-84]. A similar device, the Visulex™ Delivery System, was designed by Aciont Inc. (Salt Lake City, Utah, USA) who is currently recruiting participants for Phase 1 and 2 clinical trials to determine the safety and efficacy of Dex sodium phosphate (DSP)-Visulex for the treatment of uveitis [85-87]. Visulex has a scleral-lens shaped applicator which improves drug delivery efficiency by maintaining and sealing the drug reservoir in place and minimizing drug clearance from the ocular surface. Even macromolecules including Immunoglobulin G (IgG) [88] and Bev [89], have been delivered transsclerally using Visulex with the same concentrations achieved in retina and choroid as with intravitreal injection.

3.1.3. Delivery approaches using iontophoresis

3.1.3.1. Transcorneal iontophoresis

Transcorneal iontophoresis has been widely investigated over the last decades **(Table 2)** as it weakens the corneal barrier, permits drugs to be delivered into the anterior segment, and provides potential in the treatment of various anterior segment diseases such as keratitis, dry eye, and corneal ulcers.

A number of antibiotics are ideal permeant candidates due to their charged chemical structure and low MW. Gentamicin and ciprofloxacin, for example, have been delivered successfully into the anterior chamber by transcorneal iontophoresis with minimal irritation with much higher drug concentrations determined in cornea and aqueous humor compared to the application of conventional topical eye drops [78, 90-92]. Steroids in their base from, on the other hand, have not been studied intensively as permeants using transcorneal iontophoresis due to the limited electroosmosis, while Dex sodium phosphate achieved a 30-fold enhancement in corneal drug concentration after cathodal iontophoretic treatment (1 mA, 1 min) using the Visulex system compared to frequent eye drop instillation (every 5 min for 1 h) [79]. Beta-blockers with various *n*-octanol/water apparent distribution coefficients have also been common permeants for evaluation of the effect of drug characteristics on iontophoretic efficacy with the permeation enhancing effect being much more pronounced for hydrophilic compared to lipophilic molecules. This was mainly attributed to the disruption of the lipophilic corneal epithelium, which constitutes the main obstacle to permeation of hydrophilic drugs [93].

Iontophoresis has also been applied to deliver macromolecules (e.g. siRNA and oligodeoxynucleotides (ODNs)) transcorneally. Phosphorothioate ODNs were successfully transferred into the anterior chamber of rabbit eyes within 5 min, into the vitreous within 10 min, and into the retina within 20 min after cathodal iontophoretic treatment (1.5 mA) without any degeneration or inflammation caused by the procedure [94]. Moreover, dextrans with different MWs (4 to 70 kDa) were transported into the cornea using anodal and cathodal iontophoresis (0.5 mA, 1 min) with the successful delivery of dextrans up to 70 kDa suggesting that iontophoresis could facilitate transcorneal delivery of macromolecules with molecular sizes larger than most siRNA [95].

Although iontophoresis improves drug penetration efficiency into the eye, the rapid clearance from the ocular tissues results in the necessity of frequent iontophoretic treatment which may increase the potential of side effects and complications [61]. To sustain drug release and maintain therapeutic concentrations at the target site over prolonged periods, transcorneal iontophoresis has recently been combined with the delivery of nanocarriers. Rabbit corneas were treated with iontophoresis (1.5 mA, 5 min) using charged nanoparticle (20 to 45 nm) loaded hydrogels. The transcorneal permeability was significantly enhanced by the surface charge of the particles with negatively charged particles showing fast uptake into the outer ocular tissues (e.g. cornea and conjunctiva) 30 min after cathodal iontophoresis, followed by rather slow migration into the inner ocular layers (e.g. ciliary body and iris) within 12 h post treatment. Positively charged particles delivered by anodal iontophoresis, on the other hand, exhibited stronger permeability into the inner ocular tissues compared to negatively charged ones, indicating that the positive charge contributed to electrostatic interactions with the negatively charged cornea, and thus increased residence time and subsequently drug uptake [81]. Recently, the feasibility of charged polyamidoamine (PAMAM) dendrimers (~50 nm) in association with iontophoresis was also explored for delivery of Dex into and across the cornea. Two dendrimers with opposing charges were investigated in this study. PAMAM G3.5, having 64 carboxyl surface groups, was used as the anionic dendrimer, while PAMAM G4, possessing 64 primary amines on the surface, was used as the cationic dendrimer. Compared with passive delivery, iontophoresis enabled both free Dex and Dex-PAMAM complexes to penetrate deeply into the cornea thereby increasing the drug concentration in the aqueous humor by 2 and 2.5 folds for free Dex and Dex-PAMAM G4 complexes, respectively, by anodal iontophoresis, and 6.6 folds for Dex-PAMAM G3.5 complexes by cathodal iontophoresis [60]. Also, Dex-PAMAM complexes achieved sustained drug release with the Dex-PAMAM G3.5 formulation showing a 90-fold decrease in the diffusion coefficient due to the strong interaction of the dendrimer with lipophilic Dex. Therefore, iontophoresis of nanocarriers in the eye is a promising strategy to enhance drug delivery and maintain therapeutic concentrations.

Table 2. Summary of permeant properties and experimental conditions using transcorneal iontophoresis.

Permeant	Molecular Size	Lipophilicity	Charge (pH 7.4)	Electrode	Current (mA)	Density (mA/cm^2)	Duration (min)	Model	Ref.
Gentamicin sulfate	576 Da	Hydrophilic	+	+	1.0	5.1	1	*In vivo* rabbit	[78]
	576 Da	Hydrophilic	+	+	0.1, 0.3, 0.6	0.51, 1.5, 3.1	1	*In vivo* rabbit	[92]
	576 Da	Hydrophilic	+	+	0.2, 0.5	0.8, 2	1	*In vivo* rabbit	[91]
Ciprofloxacin hydrochloride	386 Da	Hydrophilic	+	+	0.48, 0.96, 1.92, 4	0.75, 1.5, 3.0, 6.25	1, 3, 5	*Ex vivo* porcine cornea	[90]
	386 Da	Hydrophilic	+	+	2.5	6.25	5	*Ex vivo* porcine whole eye	[90]
DSP	516 Da	Hydrophilic	-	-	1.0	5.1	1, 4	*In vivo* rabbit	[79]
Dex	392 Da	Lipophilic	-	-	0.8	1	180	*Ex vivo* porcine cornea	[60]
	392 Da	Lipophilic	-	-	4.08	5.1	4	*In vivo* rabbit	[60]
Timolol maleate	432 Da	Hydrophilic	+	+	0.5	0.64	0.5	*In vivo* rabbit	[93]
	432 Da	Hydrophilic	+	+	1.0	1.28	0.5, 5	*In vivo* rabbit	[93]
	432 Da	Hydrophilic	+	+	2.0	2.56	5 (RT), 10 (ST)	*In vivo* rabbit	[93]
	432 Da	Hydrophilic	+	+	5.0	6.41	10 (ST), 40 (ST), 10 (RT)	*In vivo* rabbit	[93]
Betaxolol hydrochloride	344 Da	Hydrophilic	+	+	0.5	0.64	0.5	*In vivo* rabbit	[93]
	344 Da	Hydrophilic	+	+	1.0	1.28	0.5, 5	*In vivo* rabbit	[93]
	344 Da	Hydrophilic	+	+	2.0	2.56	5 (RT), 10 (ST)	*In vivo* rabbit	[93]
	344 Da	Hydrophilic	+	+	5.0	6.41	10 (ST), 40 (ST), 10 (RT)	*In vivo* rabbit	[93]
Lidocaine hydrochloride	288 Da	Hydrophilic	+	+	0.22, 0.44, 0.88, 2.2	0.5, 1.0, 2.0, 5.0	30	*Ex vivo* rabbit cornea	[96]
Sodium benzoate	144 Da	Hydrophilic	-	-	0.22, 0.44, 0.66, 0.88	0.5, 1.0, 1.5, 2.0	30	*Ex vivo* rabbit cornea	[96]
Dextrans	4, 20, 70 kDa	Hydrophilic	0	+	0.5	25	1	*In vivo* mice	[95]
	4, 20, 70 kDa	Hydrophilic	0	+/-	2	100	0.167	*In vivo* mice	[95]
	4.4 kDa	Hydrophilic	0	+	0.22, 0.44, 0.88, 2.2	0.5, 1.0, 2.0, 5.0	30	*Ex vivo* rabbit cornea	[96]
GAPDH siRNA	~ 13 kDa	Hydrophilic	-	+/-	0.5	25	1	*In vivo* mice	[95]
S-ODNs	NA	Hydrophilic	-	-	1.5	N	5, 10, 20	*In vivo* rabbit	[94]
ODNs	~ 7 kDa	Hydrophilic	-	-	0.3	1.1	5	*In vivo* rat	[97]
	NA	Hydrophilic	-	-	0.5	1	4	*In vivo* rat	[98]
Nanoparticles	20 nm	NA	-	-	1.5	6	5	*In vivo* rabbit	[81]
	45 nm	NA	+	+	1.5	6	5	*In vivo* rabbit	[81]
Dendrimers	54 nm	NA	-	+/-	0.8	1	180	*Ex vivo* porcine cornea	[60]
	48 nm	NA	+	+	0.8	1	180	*Ex vivo* porcine cornea	[60]

	54 nm	NA	-	-	4.08	5.1	4	*In vivo* rabbit	[60]
	48 nm	NA	+	+	4.08	5.1	4	*In vivo* rabbit	[60]

GAPDH-Glyceraldehyde-3-phosphate dehydrogenase; RT-Repeated treatment with 30 min intervals; ST-Single treatment; NA-Not available.

3.1.3.2. Transscleral iontophoresis

Transscleral iontophoresis overcomes the lens-iris barrier and delivers drugs directly into the retina via the sclera and the choroid. As a potential alternative to intravitreal injection, transscleral iontophoresis may provide more efficient treatment of posterior segment disorders in a minimally or non-invasive fashion (**Table 3**).

Small molecules, including antibiotics [99], anti-metabolics [100], β-blockers [101], and steroids [67], have been transported iontophoretically in a reproducible and controlled manner into the retina and choroid with only a few side effects compared to conventional intravitreal injection. Transscleral iontophoresis has also been used to transport macromolecules such as monoclonal antibodies [59], IgG [102], ODNs [103], and plasmid DNA [104] to the posterior segment without breaking their structural integrity or losing their physiological function. Pescina et al. [103] reported that the transscleral permeability coefficients of three single stranded ODNs (ssDNA; MW ~ 4.2, 7.9, and 11.5 kDa) increased four folds using cathodal iontophoresis compared to passive transport without substantial differences amongst the three ssDNA. This could be due to the fact that charged macromolecules such as proteins and nucleic acids can adopt complex secondary and tertiary structures [105], which may affect the charge density, shape, and hydrodynamic radii of the molecules. Thus, MW was not considered the deciding factor for transscleral diffusion of ODNs. Repeated iontophoretic delivery of a plasmid targeted to the photoreceptor layer as a potential strategy to treat retinal degeneration was also investigated. Consecutive cathodal iontophoresis (200 μA, 5 min; 300 μA, 5 min; 400 μA, 10 min) was employed to transport cGMP-phosphodiesterase β-subunit (β-PDE) cDNA into the eye which partially rescued photoreceptors morphologically and functionally [104]. More recently, the effects of anodal and cathodal iontophoretic (2 mA, 2 to 96 h) transscleral transport of BSA (MW 66 kDa), PSS (MW 67 kDa), and Bev (MW 149 kDa) were also determined, with substantial differences in permeability seen due to the different molecular size and charge. It was therefore concluded that proteins of up to 150 kDa can successfully be delivered via anodal iontophoresis, while highly negatively charged macromolecules such as ODNs and siRNA may only be effectively transported using cathodal iontophoresis [59].

Exploiting the surface charge of the delivery system, nanoparticles were also electrically repulsed into posterior segment tissues within the first 30 min post transscleral iontophoresis (1.5 mA, 5 min) with the electrode carrying the same charge as the nanoparticle surface, providing evidence that the iontophoretic transport of unionized poorly permeable drugs can be improved by incorporation into

charged nanoparticles [81]. Negatively charged micelles were also combined with iontophoresis as a promising strategy for the treatment of chronic ocular disorders. Dex was encapsulated into the micelles to achieve sustained drug release and increase the solubility of the poorly water-soluble steroid. Drug-loaded micelles were then efficiently delivered into and across the sclera using anodal and cathodal iontophoresis (2 mA, 20 min) [61]. The combination of micelles and iontophoresis hereby maintained a high local drug concentration over a prolonged period and sustained the overall drug release, thus improving the therapeutic efficacy and avoiding frequent administration. However, the safety of the proposed micelles for transscleral iontophoretic delivery needs further investigation with regards to ocular irritation and toxicity.

Table 3. Summary of permeant properties and experimental conditions using transscleral iontophoresis.

Permeant	Molecular size	Lipophilicity	Charge (pH 7.4)	Electrode	Current (mA)	Density (mA/cm^2)	Duration (min)	Model	Ref.
Amikacin	585 Da	Hydrophilic	+	+	2, 3, 4	3.70, 5.56, 7.40	20	*In vivo* rabbit	[84]
Vancomycin hydrochloride	1486 Da	Hydrophilic	+	+	0.5, 1.0, 2.0	2.55, 5.1, 10.2	120	*Ex vivo* rabbit sclera	[101]
Gentamicin sulfate	576 Da	Hydrophilic	+	+	1	5.1	2 (×2)	*In vivo* rabbit	[99]
Acetylsalicylic acid	180 Da	Hydrophilic	-	-	2.5	5	10	*In vivo* rabbit	[106]
Carboplatin	371 Da	Hydrophilic	+	+	NA	2.57	5	*In vivo* mice	[100]
Methotrexate	454 Da	Hydrophilic	-	-	1	1.6	2 (a)	*In vivo* rabbit	[107]
	454 Da	Hydrophilic	-	-	1	5	5 (a)	*In vivo* rabbit	[107]
Timolol maleate	432 Da	Hydrophilic	+	+	0.5, 1.0, 2.0	2.55, 5.1, 10.2	120	*Ex vivo* rabbit sclera	[101]
Manganese ions	55 Da	Hydrophilic	+	+	1, 2	2.38, 4.76	10	*In vivo* rabbit	[76]
	432 Da	Hydrophilic	+	+	4	4	5	*In vivo* rabbit	[101]
DSP	516 Da	Hydrophilic	-	-	0.5, 1.0, 2.0	2.55, 5.1, 10.2	120	*Ex vivo* rabbit sclera	[101]
	516 Da	Hydrophilic	-	-	2, 4, 6	2, 4, 6	5	*In vivo* rabbit	[101]
	516 Da	Hydrophilic	-	-	1	5.0	2 (×2)	*In vivo* rabbit	[79]
	516 Da	Hydrophilic	-	-	NA	NA	NA	*In vivo human*	[85-87]
EGP-437	516 Da	Hydrophilic	-	-	Various	Various	Various	*In vivo human*	[68-74]
Balanced salt solution	NA	Hydrophilic	NA	+/-	0.1, 0.5, 1, 2, 3, 4	NA	20, 40	*In vivo human*	[82-84]
Methylprednisolone hemisuccinate sodium salt	497 Da	Hydrophilic	-	-	1, 2.4, 4.8, 7.2	1.67, 4, 8, 12	5	*Ex vivo* porcine sclera	[67]
	497 Da	Hydrophilic	-	-	2.4	4	2, 5, 10, 15	*Ex vivo* porcine sclera	[67]
	497 Da	Hydrophilic	-	-	1	2.6	5 (a)	*In vivo* rabbit	[80]
	497 Da	Hydrophilic	-	-	1	2.6	10 (b)	*In vivo* rabbit	[80]
ssDNA	~ 4.2, 7.9, 11.5 kDa	Hydrophilic	-	+/-	1.75	3	120	*Ex vivo* bovine	[103]

								sclera	
	~ 7.9 kDa	Hydrophilic	-	+/-	3.0	5	120	*Ex vivo* bovine sclera	[103]
Plasmid DNA	NA	Hydrophilic	-	-	0.3, 0.6	NA	15	*In vivo* mice	[104]
PSS	67 kDa	Hydrophilic	-	+/-	2	10	120-5760	*Ex vivo* human sclera	[59]
IgG	~150 kDa	Hydrophilic	-	+	4, 8	1.8, 3.6	20	*In vivo* rabbit	[88]
Bev	149 kDa	Hydrophilic	-	+/-	2	10	NA	*Ex vivo* human sclera	[59]
	149 kDa	Hydrophilic	-	+	NA	1.8	20	*In vivo* rabbit	[89]
	149 kDa	Hydrophilic	-	+/-	2.3	3.8	120	*Ex vivo* human sclera	[102]
BSA	68 kDa	Hydrophilic	-	+/-	2	10	NA	*Ex vivo* human sclera	[59]
Galbumin™	80 kDa	Hydrophilic	-	-	4	57.1	20	*In vivo* rabbit	[108]
Dextrans	39 kDa	Hydrophilic	0	+	0.3, 1.0, 1.75, 3.0, 4.2	0.5, 1.67, 2.92, 5, 7	120	*Ex vivo* porcine sclera	[109]
	39 kDa	Hydrophilic	0	+	4	1.07	30, 120	*Ex vivo* porcine whole eye	[109]
	4.4, 39, 120 kDa	Hydrophilic	0	+/-	1.75	2.9	2	*Ex vivo* porcine sclera	[65]
	120 kDa	Hydrophilic	0	+	1.75	2.9	2	*Ex vivo* human sclera	[65]
Cytochrome c	12.4 kDa	Hydrophilic	+	+	0.9, 1.75, 3.5	1.5, 2.9, 5.8	120	*Ex vivo* porcine sclera	[9]
Nanoparticles	20 nm	NA	-	-	1.5	6	5	*In vivo* rabbit	[81]
	45 nm	NA	+	+	1.5	6	5	*In vivo* rabbit	[81]
Micelles	4.6, 5.1, 5.3 nm	NA	-	+/-	2	10	20	*Ex vivo* human sclera	[110]
	4.4, 4.7 nm	NA	-	+/-	2	10	20	*Ex vivo* human sclera	[61]

a-Treated at two opposite sites; b-Treated at the same site; ×2-Treated twice; NA-Not available

3.2. Electroporation

Electroporation relies on a relatively high intensity electrical field, typically over 100 V/cm, and a short pulse duration (micro- to milliseconds). These conditions induce reversible destabilization and transient permeabilization of cellular barriers enabling easier access of drugs and genetic materials to ocular cells and tissues [111]. Unlike iontophoresis which has been investigated in clinical trials and is close to commercialization, electroporation used for drug and gene delivery is relatively new and is still being actively researched in pre-clinical models [112].

3.2.1. Underlying mechanisms of electroporation

In general, when an external electrical field is applied to a biological membrane, cellular transmembrane potentials increase due to the generation of aqueous pores within nanoseconds. The permeant is then transported through these pores mainly by diffusion with some contributions from electrophoresis and electroosmosis (**Fig. 3**). Previously, destabilization and electroporative elongation of cells along the axis of the electrical field were considered the main factors leading to conical hydrophilic pore formation [113]. Under the continuing influence of the external electrical field and at a given cell permeation threshold [114], pores coalesced resulting in enlarged hydrophilic pores [115]. Recently, computational studies based on molecular dynamics have become a powerful tool to understand the process of pore formation by simulating lipid bilayers in the presence of an external electrical field giving detailed insight into the process of electroporation, including mechanisms and time of pore formation [116-118]. Tarek [119] investigated the formation of water channels using dimyristoyl-phosphatidylcholine (DMPC) and palitoyl-oleyl-phosphatidylcholine (POPC) bilayers. Electric fields (0.5 and 1.0 V/nm) were applied to induce electroporation of the lipid bilayer manifested by the formation of water channels across the membrane. Dipalmitoyl-phosphatidyl-choline (DPPC) membranes were also selected as a model to study the time of pore formation with results indicating that nanoscale pores could typically be formed within 5 to 6 ns for a spatially averaged external field of 0.01 V/nm [118]. Although several models are available to predict the size and spatial distributions of pores, the molecular basis of pore formation remains poorly understood [119-121].

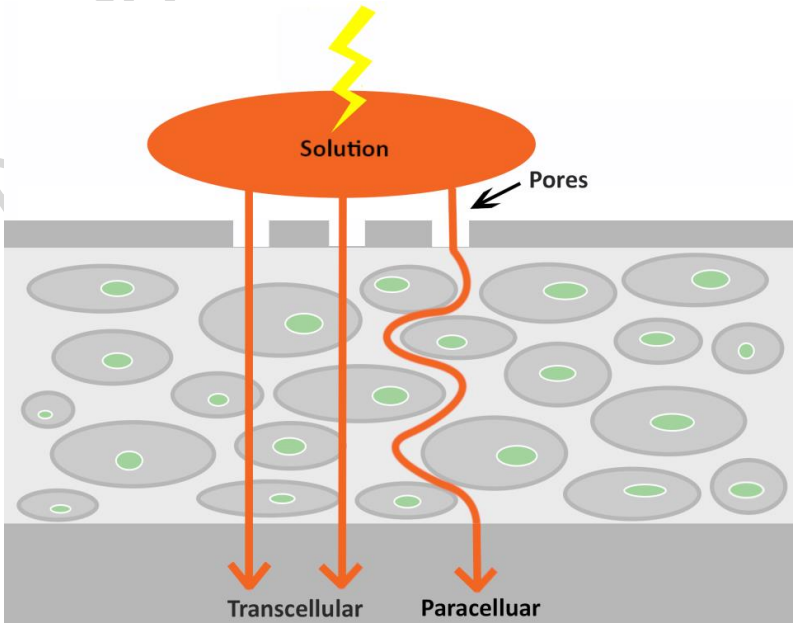

Fig. 3. Permeant transport into the target tissue through pores created by electroporation.

3.2.2. Delivery approaches using electroporation

Parameter optimization is a critical issue when translating electroporation into practical applications. When high electrical voltages and extended electric pulses are applied, tissue damage may occur by overheating cells or by irreversible dielectric breakdown, which is generally associated with necrosis [122]. Therefore, electroporation parameters (electrode dimensions, field strength, and pulse duration) need to be carefully adjusted based on the specific target tissue in order to obtain optimal efficacy while avoiding side effects. It is commonly believed that an average of 6 to 10 pulses of 20 to 40 ms with a field strength in the order of 100 to 200 V/cm is optimal for tissue electroporation in *in vivo* studies [123]. Although longer pulse durations can lead to the creation of larger pores that stay open for longer, thus favoring transfection efficacy [124], they may also cause substantial damage to the treated tissue.

Previous publications referring to the application of electroporation in the ophthalmic field have mainly focused on gene transfection. Plasmids were injected intracorneally or subconjunctivally and square-wave electric pulses were immediately applied to deliver eight pulses of 10 ms duration each to the eye at varying field strengths (100, 200, and 400 V/cm). Up to 1000-fold more gene products were transfected by the application of electric pulses compared with injection of DNA alone. No side effects were observed at the optimal field strength of 200 V/cm; however, corneal damage occurred at higher field strengths [125].

The effects of electroporation (20 V intensity, 8 pulses, 50 ms duration, 1 s intervals), iontophoresis (0.5 mA, 1 min), or a combination of both were also evaluated for delivering a highly negatively charged macromolecule, GAPDH siRNA (MW ~13 kDa), into the cornea of mice. Although both electroporation and iontophoresis applied alone enabled macromolecule transport into the cornea, the combination resulted in much higher penetration efficiency, as cathodal iontophoresis drove the negatively charged siRNA into the epithelium while electroporation further assisted the delivery by transiently permeabilizing the cell membrane. Moreover, this combination did not seem to cause any corneal damage, illustrating the feasibility and safety of electrically assisted delivery of macromolecules into the cornea [95].

Suprachoroidal electrotransfer has also been developed as a novel ocular transfection method. The delivery of non-viral plasmid DNA into the suprachoroidal space (SCS) was improved with the application of cathodal electroporation with an electrical field strength of 40 V/cm. A significant inhibition of laser-induced choroidal neovascularization was achieved within 15 days after transfection of a vascular endothelial growth factor receptor-1 encoding plasmid and no obvious retinal disorganization or gross structural damage in eyes treated with electrotransfer were detected.

Thus, combination of gene therapy with a physical method may provide a new prospect in the treatment of genetic retinal diseases [126].

4. Sonophoresis

Sonophoresis, also called ultrasound (US), involves the application of a sound field at frequencies higher than 20 kHz to improve drug transport across biological membranes, including ocular barriers [127]. US is applied over the tissue through a coupling medium which enables the propagation of the acoustic field [128]. US has been utilized in ophthalmology for decades but mostly as a diagnostic imaging tool [129]. Recently, therapeutic US has emerged as an option to treat glaucoma by cyclocoagulation [130] or enhance ocular uptake of molecules such as low MW drugs [131], genes [132], and proteins [133].

4.1. Underlying mechanisms of sonophoresis

The mechanisms for US enhanced drug delivery include non-thermal (e.g. cavitation, acoustic streaming, and mechanical stress) and thermal effects. US parameters, co-administration of microbubbles (MBs), and drug-related characteristics may all affect US mediated delivery [131, 133]. And while the efficacy of US mediated ocular drug delivery has been confirmed and a few mechanistic studies have been undertaken, the dominant contribution of US in inducing a therapeutically relevant bio-effect remains unclear. As human eyes are extremely sensitive, it is incredibly important to keep a good balance between the efficacy and safety of the applied US. Additionally, a clear understanding of the US mechanisms and precise monitoring of mechanically induced bio-effects (e.g. temperature increase and cavitation regulation processes) can avoid potential side effects to the eye thus suggesting US mediated ocular drug delivery as a safe and minimally or non-invasive technique [134].

Cavitation is generally considered the predominant factor in the enhancement of drug delivery by US (**Fig. 4**) [135]. It is defined as the cavity activity and formation of MBs due to an acoustic pressure gradient within the acoustic coupling medium. The continuous pulsation of cavitation MBs in the US field over many pressure cycles without collapse is considered stable cavitation, which can cause rupture of the membrane [136]. A dramatic growth of MBs, however, may lead to a fierce collapse within a few pressure cycles and generate pits on the surface of the membrane [137]. This cycle of growth and collapse is associated with inertial cavitation which has also shown to alter ocular barrier properties in drug delivery [127]. Corneal permeability enhancement is considered a result of cavitation with stable cavitation being the only mechanism at low US intensities, whereas both stable and inertial cavitation play important roles at higher US strengths [127]. Transscleral US-assisted

delivery is also attributed to cavitation by creating more transport channels and non-covalently modifying the proteoglycan fiber morphology without significantly disturbing the collagen network of the sclera. Low intensity US produces sufficient acoustic pressure to generate stable oscillating MBs and induces microstreaming; however, much higher intensities are required to achieve inertial cavitation [133, 138].

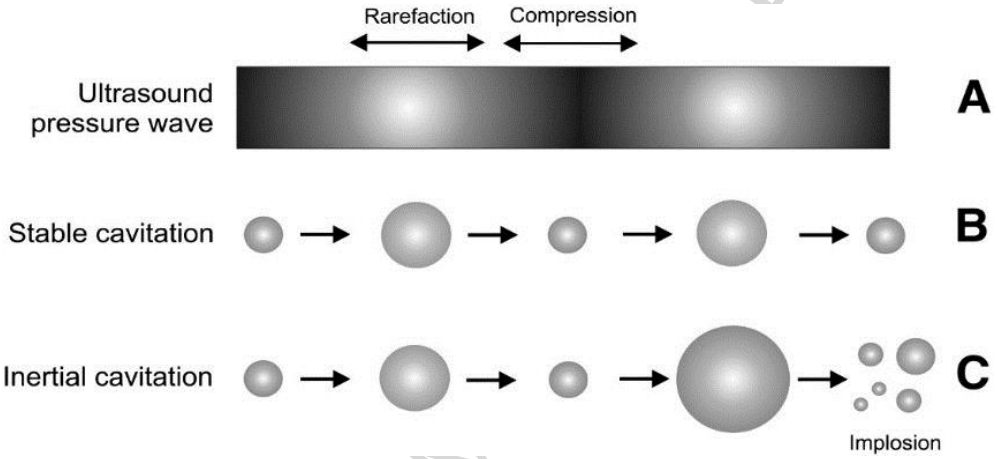

Fig. 4. Schematic of stable and inertial cavitation. (A) An acoustic pressure wave, (B) stable cavitation and (C) inertial cavitation. Image adapted from [139].

When an US wave travels through a medium, a part of its energy is absorbed, which leads to an energy and pressure gradient. In fluids, this gradient creates a flow called acoustic streaming, which in turn exerts shear stress on the biological membranes [140]. The role of the bulk flow due to acoustic streaming has been investigated in preliminary studies and evidence shows that although acoustic streaming is not as strong as microstreaming generated by oscillating MBs, the corresponding shear stress results in an enhancement of both of transcorneal and transscleral drug delivery [127, 131, 141].

Mechanical stress occurs due to the induction of sinusoidal pressure variations in a medium by a longitudinal US wave. This wave has a direct influence on cells and tissues and causes density variation in them, resulting in cyclic stress and leading to fatigue. However, the role of mechanical stress has not yet been clarified for ophthalmic applications. Under US of 20 kHz, the mechanical stress can be neglected for the permeability variation across the cornea, since the wavelength of the incident beam (~7.5 cm) is much greater than the thickness of the cornea (~0.5 mm). Thus, a significant gradient in the net pressure across the cornea is not expected [142]. Cheung et al. [133] also pointed out that the mechanical stress in US mediated transscleral delivery could not explain the improvement in drug transport.

With US application, the temperature of the applied tissue might increase due to absorption of sound waves with a higher absorption coefficient of the respective tissue leading to a greater temperature

increase and thus a stronger thermal effect which has also been correlated with the enhancement of drug permeability. For example, the corneal permeability of ophthalmic agents such as tobramycin and DSP was enhanced with a temperature change from 34 to 37 °C after US exposure (0.4 to 1 MHz, 0.3 to 1.0 W/cm^2, 5 min) [131]. However, this temperature increase and overheating of ocular tissues by US application for enhanced drug delivery is a major concern in the clinical setting [143-145]. For US diagnosis, the thermal safety requirements allow a maximal temperature increase of 1.5 °C [146]. Therefore, researchers have to carefully select US conditions at low energy levels to limit any excessive temperature increase and thus tissue damage.

4.2. Delivery approaches using sonophoresis

4.2.1. Transcorneal ultrasound

US enhanced transcorneal drug delivery has been investigated for various drugs. A hydrophilic dye was initially delivered through a rabbit cornea under US exposure (880 kHz, 0.19 to 0.56 W/cm^2, 5 min) and an up to ten-fold increase in dye concentration in the aqueous humor was observed [127]. A few ophthalmic agents such as tobramycin and DSP were subsequently delivered to evaluate the influence of various US waves (0.4 to 1.0 MHz, 0.3 to 1.0 W/cm^2, 5 min) on the corneal barrier properties and drug permeability. Although these compounds had similar molecular properties, the permeability of tobramycin without or with US exposure did not change, while the permeability of DSP significantly increased after US exposure. Therefore, no conclusions could be drawn regarding the effect of molecular properties on US enhanced transcorneal drug delivery with further studies required to identify the factors affecting US mediated delivery [131]. Overall, the optimal efficiency of transcorneal US mediated delivery is closely associated with the US parameters (e.g. frequency and intensity). When lower frequency US (20 kHz) was employed, the enhancement in transcorneal transport, unlike the significant increase observed in transdermal delivery, was less than that achieved by US of medium frequencies (660 to 880 kHz), although a ten-fold higher intensity and a 12-fold longer exposure duration were used. Therefore, low frequency 20 kHz US was deemed unsuitable in the case of transcorneal delivery with further investigations required to determine the increase in transcorneal permeability caused by US of various parameter settings [142].

Overall, a combination of US and MBs has been thought to be a more effective approach to deliver drugs and genes into the ocular tissues. MBs were originally developed as US contrast agents to improve ultrasonographic images. Based on the results from mechanistic studies, US increases the permeability of biological membranes by generation of MBs which act as cavitation nuclei, effectively focusing US energy and leading to higher image contrast. Thus, it was found that the required US energy could be greatly reduced in the presence of MBs [147]. In terms of ocular drug delivery, the majority of studies referring to a combination of US and MBs have focused on gene

transfection. For example, *p*EGFP-N2, a green fluorescent protein plasmid, was injected into the rabbit cornea *in vivo* together with MBs (20% w/v) followed by US application (1 MHz, 1 to 2 W/cm^2, 120 s, 50% duty cycle). While plasmid DNA injection alone only provided limited gene transfer, plasmid DNA injection with MBs plus US significantly increased gene transfer efficiency without apparent tissue damage with gene expression mainly in the area exposed to US [148].

4.2.2. Ultrasound mediated delivery to the posterior segment

Studies on the application of US enhanced drug delivery to the posterior segment are rather limited (**Table 4**). Due to the unique barrier properties of the eye, it is necessary to develop and validate an effective approach with regards to US parameters and permeability kinetics in order to transport drugs efficiently and without any safety concerns into the posterior segment.

US mediated *ex vivo* transscleral delivery of macromolecules was investigated by determining BSA transport through rabbit sclera after US exposure (1 MHz, 0.05 W/cm^2, 30 s) resulting in 1.6-fold higher BSA concentrations without causing any damage to the retinal tissues [133]. The *in vivo* efficacy of transscleral US was subsequently evaluated at a much lower frequency (40 kHz, 0.12 W/cm^2, 90 s). Results indicated that low frequency US significantly increased the penetration of macromolecules via the transscleral route with good tolerability [10]. Recently, a novel macromolecular delivery approach was developed by combining transscleral US with nanocarriers. US application (1 MHz, 0.5 W/cm^2, 5 min) considerably enhanced the penetration efficiency of BSA loaded nanoparticles through *ex vivo* rabbit sclera, meanwhile nanocarriers enabled sustained drug release, which in turn would reduce the need for frequent administration and US application [149]. Similarly, transscleral US (1 MHz, 0.5 W/cm^2, 30 s) was also utilized to enhance the vitreous diffusivity and retinal permeability of peptide loaded nanoparticles following intravitreal injection in order to achieve higher retinal drug concentrations [150]. No safety issues due to US application were reported in these studies with the ocular tissues showing normal morphology and the temperature rise being below the maximal limit of 1.5 °C for US application in ophthalmology [146].

High intensity focused ultrasound (HIFU), a clinically applicable tool in the treatment of glaucoma [130, 151-153], has also recently been tested for transscleral drug delivery. One hundred HIFU pulses with a pulse duration of 50 ms and a pulse repetition frequency of 1 Hz increased the penetration depth of two model drugs, bicinchoninic acid and rhodamine 6G, by 2.0- and 3.1-fold, respectively, which indicated that HIFU may be an effective modality for transscleral drug delivery with a high transporting rate and depth. No morphological changes were found in the sclera after HIFU if the pulse duration was shorter than 50 ms while temperature elevation was also negligible (< 1 °C). However, erosion on the scleral surface was observed after HIFU with pulse durations longer than 100 ms, which was due to the subcellular tissue fragmentation by bubble cavitation. In addition to

small molecules, macromolecules and controlled release systems (e.g. liposomes and nanoparticles) may also be suitable for HIFU mediated delivery, as US has no special requirement with regards to permeant properties (e.g. charge and lipophilicity), although particle size is considered the major factor affecting penetration efficiency [154].

US co-administration with various gaseous particles, such as liposomes, bubble liposomes, and MBs, has also been applied for drug and gene delivery to the posterior segment of the eye [155]. It is worth mentioning here that in addition to being the causative agents for barrier disruption, these formulations can also serve as drug delivery vehicles stably carrying drugs and genes into biological tissues. Drugs and genes can hereby be adsorbed onto or embedded into the shell matrix or encapsulated in the internal gaseous core [156].

Non-viral gene nanoparticles, including PEGylated polystyrene nanospheres and non-PEGylated lipoplexes, were formulated and co-delivered *ex vivo* through bovine retina under US (1 MHz, 0.5 to 1 W/cm^2, 30 to 120 s, 50 to 100% duty cycle) to facilitate nanoparticle uptake by RPE cells. However, longer durations were necessary to improve the permeation of larger sized nanoparticles through the neural retina, underlining the importance of developing small sized carriers (< 130 nm) for the delivery of nucleic acids to the neural retina and the RPE [157]. More recently, US-targeted MB destruction (1 MHz, 2 W/cm^2, 5 min, 50% duty cycle) was utilized to enhance and accelerate transgene expression in the retina by transferring rAAV2-CMV-EGFP, a viral vector encoding a plasmid DNA, through the sclera and vitreous into the subretinal space of rats. Here, the gene expression was much higher than that of other groups (AAV, AAV+MBs, and AAV+US) before day 35; however, there was no difference between these formulations after 35 days. A possible explanation was that US created transient pores immediately after exposure and provided another pathway for AAV to enter thereby facilitating AAV delivery into the cells through US-targeted MB destruction with higher amounts delivered than those by natural transfection [158].

So far, there has been no evidence that US can enhance retinal permeability upon extraocular administration in large animal models. In addition, the lack of retinal targeting of extraocularly applied US may result in unpredictable effects in other ocular tissues. Focused retinal US application, on the other hand, is expected to result in higher delivery efficiency and minimize damage to the surrounding tissues. A tiny intravitreal US transducer as small as a 19G needle was therefore designed which delivered US (3 MHz, 0.15 W/cm^2, 60 s, 6% duty circle) selectively and intensively to the retina and enhanced plasmid DNA transfer efficacy [159]. This concept may be feasible to treat retinal diseases in the future. However, more *in vivo* data is needed, especially referring to the safety of the device, since intravitreal US application is rather invasive and frequent surgical procedures may be required increasing the risk of intraocular infections and other surgical complications.

Despite locally enhanced ocular drug delivery, targeted delivery of systemically administered drugs to the retina using focused US has also recently been achieved. US (10 ms bursts applied at 1 Hz for 60 s) was delivered through the cornea and lens into the retina in one rat eye along with intravenous injection of MBs, leading to transient disruption of the BRB and increasing the concentration of a MRI contrast agent (Magnevist, MW 938 Da) in the vitreous humor. This provided a non-invasive technique for retinald delivery of systemically administered drugs. With regards to safety, this study also highlighted that the risk of side effects might be reduced at low exposure levels or when utilizing a transducer that produces a small focal region [160]. **Table 4** gives an overview of recent studies on ultrasound enhanced drug delivery to the eye.

Table 4. Summary of permeant properties and experimental conditions for ultrasound mediated drug delivery to the eye.

Delivery route	Permeant	Molecular size	Lipophilicity	Charge (pH 7.4)	Frequency (MHz)	Intensity (W/cm^2)	Duration (min)	Model	Ref.
Transcorneal	Sodium fluorescein	376 Da	Hydrophilic	-	0.88	0.19, 0.34, 0.56	5	*Ex vivo* rabbit cornea	[127]
	Sodium fluorescein	376 Da	Hydrophilic	-	0.4, 0.6, 0.8, 1	1.0	5	*Ex vivo* rabbit cornea	[131]
	Tobramycin	467 Da	Hydrophilic	+	0.4, 0.6, 0.8, 1	0.5, 0.8, 1.0	5	*Ex vivo* rabbit cornea	[131]
	DSP	516 Da	Hydrophilic	-	0.4, 0.6, 0.8, 1	0.3, 0.5, 0.8, 1.0	5	*Ex vivo* rabbit cornea	[131]
	DSP	516 Da	Hydrophilic	-	0.4, 0.6	0.8	5	*In vivo* rabbit	[161]
	Atenolol	266 Da	Hydrophilic	+	0.02	2	10, 30, 60	*Ex vivo* rabbit cornea	[142]
	Carteolol	292 Da	Hydrophilic	+	0.02	2	10, 30, 60	*Ex vivo* rabbit cornea	[142]
	Timolol	316 Da	Lipophilic	+	0.02	2	10, 30, 60	*Ex vivo* rabbit cornea	[142]
	Betaxolol	307 Da	Lipophilic	+	0.02	2	10, 30, 60	*Ex vivo* rabbit cornea	[142]
	pEGFP-N2	NA	Hydrophilic	-	1	0.8, 1.0 1.2	0.33, 1	*In vitro* rabbit corneal epithelial cells	[132]
	pEGFP-N2	NA	Hydrophilic	-	1	1, 2	1, 2	*In vitro* rabbit corneal epithelial cells	[148]
	pEGFP-N2	NA	Hydrophilic	-	1	1, 1.5, 2	2	*In vivo* rabbit	[148]
Subconjunctival	pEGFP-N2	NA	Hydrophilic	-	1	1.2	0.33	*In vivo* rat	[132]
Transscleral	BSA	65 kDa	Hydrophilic	-	1, 3	0.05	0.5	*Ex vivo* rabbit whole eye	[133]
	BSA	65 kDa	Hydrophilic	-	0.04	0.002, 0.01, 0.05, 0.38, 1.8	0.5	*Ex vivo* rabbit sclera	[138]
	Dextrans	70 kDa	Hydrophilic	0	0.04	0.12	1.5 (RT)	*In vivo* rabbit	[10]
	Dextrans	20, 70, 150 kDa	Hydrophilic	0	0.04, 0.5, 1, 3	0.05	0.5	*Ex vivo* rabbit sclera	[162]
	Nanoparticles	214 nm	NA	-	1, 3.3	0.5	5	*Ex vivo* rabbit sclera	[149]
	Bicinchoninic acid	344 Da	Hydrophilic	-	1.1 (PRF 1 Hz)	NA	10, 20, 50 ms bursts	*Ex vivo* porcine sclera	[154]
	Rhodamine 6G	479 Da	Hydrophilic	+	1.1 (PRF 1 Hz)	NA	10, 20, 50 ms bursts	*Ex vivo* porcine sclera	[154]
Intravitreal	pEGFP-N2	NA	Hydrophilic	-	3	0.15	1	*In vivo* rabbit	[159]

	Lipoplexes	228, 203, 115 nm	NA	+	1	0.5, 1	0.5, 1, 2	*Ex vivo* posterior tissue of bovine eye	[157]
	Nanospheres	38, 122, 190 nm	NA	-	1	0.5, 1	0.5, 1, 2	*Ex vivo* posterior tissue of bovine eye	[157]
	Nanoparticles	252 nm	NA	-	1	0.5	0.5 (RT)	*Ex vivo* posterior tissue of bovine eye	[150]
Subretinal	rAAV2-CMV-EGFP	NA	Hydrophilic	-	1	1, 2, 3	1, 2	*In vitro* human RPE cell	[158]
	rAAV2-CMV-EGFP	NA	Hydrophilic	-	1	2	5	*In vivo* rat	[158]
Intravenous	MBs	1.1-3.3 μm	NA	-	0.69 (PRF 1 Hz)	NA	1 (10 ms bursts)	*In vivo* rat	[160]

PRF-Pulse repetition frequency; NA-Not available; RT-Repeated treatment

5. Microneedles

Microneedles (MNs) are individual needles or arrays of micrometer sized needles fabricated by adapting microelectronics tools. Applying MNs to biological membranes can create transport pathways of micro-dimensions and enhance the permeability of therapeutic agents across such membrane barriers. Numerous MN fabrication approaches have been developed in a variety of shapes, sizes, materials, and configurations [163]. Most MN studies to date have focused on transdermal delivery and have shown MNs to be large enough to pierce the skin and deliver a broad range of drugs, from small molecules to macromolecules, including peptides, genes, and vaccines [164]. To avoid side effects caused by conventional intravitreal or periocular injections, the application of MNs in ophthalmology has also been explored as a novel physical method for ocular drug delivery with various ocular MNs designed and different delivery routes evaluated.

5.1. Fabrication of microneedles

MNs used for ocular drug delivery are generally categorized into four types according to their delivery mechanism **(Fig. 5)**: (1) Solid MNs are applied as a biological membrane pretreatment, able to create micropores in the ocular surface after insertion. After removing the MNs, therapeutic agents can diffuse through the created pores into the eye. (2) Drug coated MNs are applied as vehicles to carry and deposit drugs within the eye. After insertion, the drug coating dissolves and diffuses into the eye, after which the MNs are removed. (3) Dissolving MNs enable drugs to be encapsulated into the MN matrix and release the incoporated drug through MN dissolution over time. These MNs are typically fabricated from safe and biodegradable polymers such as polyvinylpyrrolidone (PVP) and poly($_{D,\,L}$-lactide) (PLA). In this way, MNs dissolve or degrade in the inserted tissue thereby releasing the encapsulated drug in a sustained manner, while also overcoming the penetration barriers due to

their design. (4) Hollow MNs, on the other hand, can infuse pressure-driven flow of a liquid formulation, which provides a defined conduit for drug delivery into the target tissue.

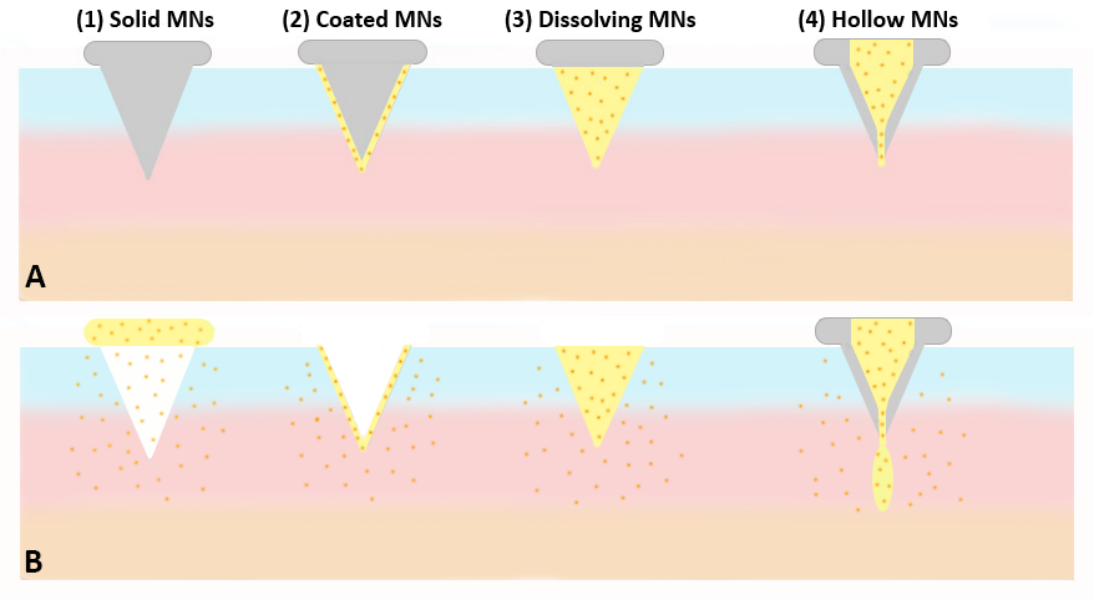

Fig. 5. MN mediated ocular drug delivery. (A) Various types of MNs are inserted into the ocular tissue and (B) drugs are delivered into these tissues by different mechanisms. Figure adapted from [164].

5.2. Delivery approaches using microneedles

5.2.1. Intracorneal delivery

Targeted drug delivery to the cornea and anterior segment of the eye can be achieved by insertion of MNs across the corneal epithelium and depositing drugs directly into the corneal stroma. Solid stainless steel MNs coated with different compounds ranging from small molecules (e.g. fluorescein and pilocarpine) to macromolecules (e.g. BSA and plasmid DNA) were fabricated and inserted into rabbit corneas *in vivo*. MNs bypassed the corneal epithelium and targeted the corneal stroma thereby providing a 60-fold higher bioavailability compared to topically administered drugs [11]. A similar result was observed in another study, in which titanium-based MNs were developed with in-plane geometry and tested in *ex vivo* rabbit corneas. These fenestrated in-plane MNs maximized the drug loading capacity per needle, therefore minimizing the total number of needles required. Moreover, they could precisely penetrate the epithelium, serving as a drug reservoir for passive delivery via diffusive transport from the fast-dissolving coating [165, 166]. Recently, MNs coated with a dry film of macromolecular Bev were designed for the treatment of corneal neovascularization to penetrate a depth of a few hundred micrometers into the corneal stroma without crossing the corneal endothelium. Eyes treated by MNs suppressed blood vessel growth efficiently with a much lower dose of Bev

compared to subconjunctival injection and topical eye drop administration thereby decreasing the possibility of side effects [167].

However, *in vivo* application of MNs to a specific region of the cornea is still challenging due to the corneal curvature and lack of a supporting pressure during MN insertion, particularly in small animals such as mice or rats. A "transfer-molding" technology has thus recently been developed which enables repetitive fabrication of MNs on the tip surface of a small rod that can be inserted into a small target region. To enhance the reliability of MN insertion, the MN pen (MNP), a spring-loaded MN applicator system, was custom fabricated, allowing easier handling of the MNs with the spring force enabling impact insertion of MNs into the target tissue with minimal damage to the MN tip. To evaluate the efficacy of MNP, sunitinib malate was delivered to mice corneas in a suture-induced angiogenesis model. It was found that sufficient drug was delivered by the MNP to inhibit corneal neovascularization in comparison to application with a 30G needle tip dipped into the drug solution [168].

5.2.2. Intrascleral delivery

The sclera is typically considered a barrier for drug transport via the periocular routes. Recently, there has been growing attention to intrascleral administration which allows drugs to be delivered more closely to the target site, especially when treating the choroid. Water soluble molecules (sulforhodamine) as well as nano- and microparticles have been injected intrasclerally using glass hollow MNs. While solutions and small nanoparticles with a size of 278 nm could be infused into intact sclera, the delivery of microparticles of 1 μm in diameter required the presence of spreading enzymes to disrupt the scleral barrier. The MN retraction procedure also affected intrascleral drug infusion, while the scleral thickness and infusion pressure had negligible effects on the volumetric delivery into the sclera [169]. In addition to drug solutions and suspensions, hollow MNs were also employed to precisely apply a thermosensitive *in situ* forming poloxamer implant into the sclera. At 20 °C the liquid poloxamer solution allowed administration through the hollow MNs, while it formed a solid implant at physiological temperature (37 °C). Temporarily formed scleral pores were recovered within 2 to 3 h after MN administration, enveloping the implant and achieving sustained drug release over 24 h by increasing the drug retention at the injection site [170].

During the MN insertion process, a suitable insertion device is generally required to fix the MNs and pierce the sclera. In a previous study, hollow glass MNs were embedded within a soft flexible poly(dimethylsiloxane) (PDMS) substrate, which could fit the contours of the ocular surface with further potential to provide control over the depth of MN insertion to the specific target layer within the eye. Also, this study used conventional microfabrication-based photolithographic techniques to

create a single replica mold that could be applied repeatedly to cast PDMS-based devices with embedded MNs in a flexible substrate [171].

Polymeric MNs have also emerged as a promising strategy for intrascleral drug delivery. Unlike solid or hollow MNs, dissolving MNs can minimize the solid material burden as well as the potential of accidental retinal damage. Moreover, they either dissolve rapidly within the inserted tissue or remain as a depot for long-term drug delivery [172]. Thakur et al. [173] developed a simple and cost-effective mouldcasting method for fabrication of rapidly dissolving MNs using PVP. Results revealed that these MNs could efficiently penetrate the outer scleral layers enhancing the intrascleral permeation of macromolecules (dextrans with a MW of 70 and 150 kDa) while rapidly dissolving within the sclera to form a drug depot. Similarly, dissolving MNs made of biodegradable PLA and loaded with 10% methotrexate were fabricated and intrasclerally applied for the treatment of primary vitreo-retinal lymphoma. In preliminary toxicity studies, the implantable MNs were inserted successfully into deep lamellar scleral pockets of rabbit eyes and permitted sustained drug release without any drug toxicity or inflammatory response [174].

5.2.3. Suprachoroidal delivery

By inserting MNs into the base of the sclera, drugs can also be delivered into the SCS, which is a potential space between sclera and choroid. Drug solutions injected into this space can flow circumferentially around the eye and may even reach the macula if the site of injection is near the limbus, which could avoid compliance issues caused by intravitreal injections and bioavailability shortcomings resulting from periocular drug delivery [164, 175].

Solutions and suspensions of 20 nm to 1 μm diameter particles have been delivered successfully into the SCS of rabbit, pig, and human eyes using hollow MNs with a maximum volume of 35 μL administered [176]. Suprachoroidal injection is influenced by the MN length, infusion and intraocular pressure, solute properties (e.g. lipophilicity and MW), and the injection site [177, 178]. When particle formulations are injected through MNs, the spread within the SCS is greatly affected by the particle size. Smaller sized particles (20 and 100 nm) exhibited extensive spread both in the sclera and SCS, while larger sized particles (500 nm and 1 μm) primarily localized in the SCS and were excluded from the sclera. Thus, for larger sized particles, longer MNs and higher infusion pressure are required [176]. A recent study also highlighted the importance of taking the anatomical barriers and injection site into account. As multiple tightly clustered vessels perforate the sclera to form a strong attachment between sclera and choroid, the circumferential spread in the SCS was significantly impeded by long posterior ciliary arteries in rabbit eyes as well as by short posterior ciliary arteries in humans. Singular large vessels (e.g. vortex veins), on the other hand, had little effect on circumferential flow [177].

Drug molecules and carriers injected into the SCS are eliminated at different rates with water soluble small molecules as well as macromolecules possessing half-lives of several hours, while nano- and microparticles can remain in the SCS for months [179]. Clearance from the SCS occurs via passive diffusion across the sclera, uptake into the choriocapillaries, and flow through scleral channels near the vortex veins. The unique sieving and clearance mechanisms allow particles to remain in the SCS until they are biodegraded into small fragments that can then be eliminated. In this way, the combination of sustained-release particles and suprachoroidal delivery using MNs can be used for sustained drug delivery for days to months [180]. In another study, non-biodegradable nano- and microparticles suspended in polymeric formulations were injected into the SCS of rabbits through hollow MNs [181]. When formulated in saline, particles were distributed over 29-42% of the SCS. The addition of hyaluronic acid resulted in moderately non-Newtonian solutions with low viscosity (~4 Pa.s) at a high shear rate (100 s^{-1}) and high viscosity (~70 Pa.s) at a low shear rate (0.01 s^{-1}) at 40 °C thereby spreading particles over larger regions (up to 100% of the SCS). Strongly non-Newtonian carboxymethylcellulose solutions, on the other hand, with low viscosity (~4 Pa.s) at a high shear rate but extremely high viscosity (~170 Pa.s) at a low shear rate limited particle spreading leading to their accumulation near the injection site adjacent to the ciliary body (8.3-20% of the SCS). This study revealed that particles injected into the SCS could be localized at the site of injection or broadly distributed throughout the SCS by controlling the viscosity of the vehicle.

Recently, suprachoroidal delivery using MNs has been evaluated in animal models of posterior segment diseases and is currently also in clinical trials. Clearside Biomedical Inc. (Alpharetta, GA, USA) evaluated the efficacy of suprachoroidal delivery using hollow MNs for the treatment of acute posterior segment uveitis by injecting triamcinolone acetonide (TA) into the SCS of live pigs. It was found that the injection of low (0.2 mg) and high (2.0 mg) doses of TA by MNs was as effective as intravitreal injection of the higher TA dose with the spreading around the eyeball primarily dependent on the injected volume [182]. The company subsequently completed a Phase 2 clinical trial (DOGWOOD) to determine the safety and efficacy of suprachoroidally administered proprietary non-preserved TA (CLS-TA (Zuprata^{TM})) via 1000 µm long MNs in subjects with macular edema associated with non-infectious uveitis and is currently recruiting participants for a Phase 3 study (PEACHTREE) for further efficacy evaluation [183, 184]. Clearside Biomedical also recently completed a Phase 2 clinical trial (TANZANITE) in subjects with macular edema following retinal vein occlusion revealing that fewer intravitreal aflibercept injections were required to achieve better visual gain with co-administration of suprachoroidal CLS-TA compared to intravitreal aflibercept alone [185]. Finally, the company is currently also investigating suprachoroidal application of a small tyrosine kinase inhibitor (Axitinib^{TM}) in the treatment of wet AMD. **Table 5** summarizes recent studies on MN mediated ocular drug delivery.

Table 5. Summary of permeant properties and experimental conditions for microneedle mediated ocular drug delivery.

Delivery route	Permeant	Molecular size	Lipophilicity	Charge (pH 7.4)	MN type	Model	Ref.
Intracorneal	Sodium fluorescein	376 Da	Hydrophilic	-	Coated MNs	*In vivo* rabbit	[11]
	Sodium fluorescein	376 Da	Hydrophilic	-	Dissolving MNs	*Ex vivo* porcine cornea	[173]
	Pilocarpine hydrochloride	244 Da	Hydrophilic	+	Coated MNs	*In vivo* rabbit	[11]
	Sunitinib malate	532 Da	Hydrophilic	+	Coated MNs	*In vivo* mice	[168]
	Sulforhodamine	606 Da	Hydrophilic	-	Coated MNs	*Ex vivo* human cornea	[11]
	Rhodamine B	479 Da	Hydrophilic	+	Coated MNs, Fenestrated MNs	*Ex vivo* rabbit cornea	[165, 166]
	Rhodamine B	479 Da	Hydrophilic	+	Coated MNs	*In vivo* mice	[168]
	Evans blue	960 Da	Hydrophilic	-	Coated MNs	*In vivo* mice	[168]
	BSA	68 kDa	Hydrophilic	-	Coated MNs	*Ex vivo* human cornea	[11]
	Bev	149 kDa	Hydrophilic	-	Coated MNs	*In vivo* rabbit	[167]
	Dextrans	70, 150 kDa	Hydrophilic	0	Dissolving MNs	*Ex vivo* porcine cornea	[173]
Intrascleral	Sulforhodamine	558 Da	Hydrophilic	-	Hollow MNs	*Ex vivo* human sclera	[169]
	Sodium fluorescein	376 Da	Hydrophilic	-	Hollow MNs	*Ex vivo* rabbit whole eye; *Ex vivo* rabbit sclera	[170]
	Sodium fluorescein	376 Da	Hydrophilic	-	Dissolving MNs	*Ex vivo* porcine sclera	[173]
	Methotrexate	454 Da	Hydrophilic	-	Dissolving MNs	*In vivo* rabbit	[174]
	Dextrans	70, 150 kDa	Hydrophilic	0	Dissolving MNs	*Ex vivo* porcine sclera	[173]
	Nanoparticles	278 nm	NA	NA	Hollow MNs	*Ex vivo* human sclera	[169]
	Microparticles	1.0 μm	NA	NA	Hollow MNs	*Ex vivo* human sclera	[169]
Suprachoroidal	β-blocker cocktail	NA	Hydrophilic	NA	Hollow MNs	*Ex vivo* rabbit whole eye	[178]
	Sodium fluorescein	376 Da	Hydrophilic	-	Hollow MNs	*Ex vivo* rabbit whole eye	[178]
	Sulforhodamine B	558 Da	Hydrophilic	-	Hollow MNs	*Ex vivo* porcine whole eye	[176]
	Sulprostone	465 Da	Hydrophilic	-	Hollow MNs	*In vivo* rabbit	[186]
	Brimonidine tartrate	442 Da	Hydrophilic	0	Hollow MNs	*In vivo* rabbit	[186]
	TA	434 Da	Lipophilic	0	Hollow MNs	*In vivo* pig	[182]
	CLS-TA	434 Da	Lipophilic	0	Hollow MNs	*In vivo* human	[183-185]
	Dextrans	4, 40 kDa	Hydrophilic	0	Hollow MNs	*Ex vivo* rabbit whole eye	[178]
	Dextrans	40, 250 kDa	Hydrophilic	0	Hollow MNs	*In vivo* rabbit	[179]
	Bev	149 kDa	Hydrophilic	-	Hollow MNs	*In vivo* rabbit	[179]
	Nanoparticles	20, 500 nm	NA	NA	Hollow MNs	*In vivo* rabbit	[179]
	Nanoparticles	20, 200 nm	NA	NA	Hollow MNs	*Ex vivo* rabbit whole eye	[181]
	Microparticles	20-45 μm	NA	NA	Hollow MNs	*In vivo* rabbit	[180]
	Microparticles	1, 10 μm	NA	NA	Hollow MNs	*In vivo* rabbit	[179]
	Microparticles	2, 10 μm	NA	NA	Hollow MNs	*Ex vivo* rabbit whole eye	[181]
	FluoSpheres	20, 100 nm	NA	NA	Hollow MNs	*Ex vivo* rabbit whole eye; *Ex vivo* porcine whole eye; *Ex vivo* human whole eye	[176]
	FluoSpheres	0.5, 1 μm	NA	NA	Hollow MNs	*Ex vivo* porcine whole eye	[176]
	FluoSpheres	20, 200 nm	NA	NA	Hollow MNs	*Ex vivo* rabbit whole eye	[177]
	FluoSpheres	200 nm	NA	NA	Hollow MNs	*Ex vivo* rabbit whole eye; *Ex vivo* human whole eye; *In vivo* rabbit	[177]
	Barium sulfate particles	1 μm	NA	NA	Hollow MNs	*Ex vivo* porcine whole eye	[176]

NA-Not available

6. Safety and tolerability

Physical force-based methods discussed above are generally considered as local, non-invasive approaches of administration associated with minimal pain or discomfort for patients. However, it should be kept in mind that the potential irritation or damage to the eye is strongly dependent on the parameter settings of each procedure and that the eye may be more sensitive to these methods than other organs such as the skin.

In general, ocular iontophoresis efficacy is primarily determined by the electric current density and duration with an increase in the applied current and time enhancing drug transport to the eye [79, 187]. However, it is believed that any toxicity is also correlated with these parameters. Transcorneal iontophoresis might affect the ocular surface, as the cornea is an avascular and highly innervated tissue, rendering it highly sensitive to pain and hypoxia. Transscleral iontophoresis, on the other hand, might distress the retina underneath the application site and thus affect normal visual function. Tolerability studies in humans have shown that the maximal current density tolerated by cornea and sclera was 1.8 mA/cm^2 for 5 min and 5.5 mA/cm^2 for 20 min, respectively [83]. Another safety concern associated with ocular iontophoresis is the risk of pH changes in the drug formulation during the procedure. Many devices used in clinical trials are integrated with inert electrodes rather than reversible electrodes with the surface electrochemistry involving the electrolysis of water, which in turn could reduce the medium pH in the anode while increasing the pH in the cathode both of which could result in ocular tissue irritation [188]. Electroporation, using higher electrical field strengths and longer pulse durations, also leads to higher drug delivery efficiency; however, significant tissue damage and inflammation can be induced [122, 125].

The safety of US mediated ocular drug delivery is also a concern, as excessive US energy can damage the eye thermally and mechanically. Thus, the Food and Drug Administration and the World Federation for Ultrasound in Medicine and Biology have imposed strict limits for the thermal (< 1.0) and mechanical indices (< 0.23) for ocular applications [189, 190]. Moreover, the European Federation of Societies for Ultrasound in Medicine and Biology considers that an US procedure is safe if the temperature increase is less than 1.5 °C above physiological levels [146]. Due to these safety limitations, a number of US mediated ocular drug delivery studies have investigated the potential damage to the eye with evidence showing that increased US frequency, intensity, and exposure duration result in a thermal elevation above the safety margins as well as structural alterations in the ocular tissues [141, 157, 161]. Recently, Nabili et al. [145] performed a modeling study to investigate the interaction between US energy and heat distribution in the eye. Results showed that US induced a higher temperature rise in the lens compared to the cornea and the optic

nerve because of its high acoustic attenuation. Thus, the pulsed mode may be a safer way to enhance ocular drug delivery with minimal heat generation to avoid overheating of the lens.

The safety of MNs for ocular delivery has also been evaluated numerically with adequate evidence showing that MNs are well tolerated *in vivo* with no significant complications such as pain, inflammation, redness, or vision loss observed [11, 174, 179, 186]. However, very little work has been done on the effect of the MN insertion forces with regards to a rise in intraocular pressure (IOP). One study on MN mediated drug delivery through the SCS measured elevation in IOP caused by the MN injection showing a transient increase in IOP that peaked at 35 ± 3 mm Hg and decayed in under 1 h, which is similar to the IOP increase induced by intravitreal injection (~30 mm Hg) [191]. Considering that conventional injection is well tolerated in patients when only topical anesthesia is applied, it is expected that the temporary increase in IOP caused by MN insertion is safe [186]. Nevertheless, further studies are needed to confirm the long-term safety of MNs and determine the recovery rate of the ocular tissues to repair the trauma caused by the MN insertion.

7. Conclusion

Achieving safe and effective treatment of ocular diseases is a challenging task due to the presence of various protective ocular barriers and elimination mechanisms. A vast number of novel strategies have been utilized to overcome these barriers and improve drug delivery to the target site thereby enhancing drug bioavailability and avoiding potential side effects. The enhancement of drug permeability, ease of application, and minimally or non-invasive characteristics render physical force-based methods an exciting strategy for the treatment of both anterior and posterior segment disorders. Iontophoresis is the most extensively investigated approach among these physical techniques so far, with numerous therapeutic agents such as low MW drugs, macromolecules, and nanocarriers successfully delivered to various ocular tissues. Although the number of studies on US and MN mediated ocular drug delivery is still limited, both have specific advantages, including site-specific drug delivery to the ocular tissues as well as the possibility to combine them with sustained release particles. Overall, such physical methods may significantly enhance drug delivery efficiency by overcoming the ocular barriers without causing detectable damage to the eye. Further *in vivo* studies are required to understand the contribution of dominant mechanisms, optimize device design and parameter settings, and evaluate the feasibility and safety of repeated and long-term application of such methods in the clinical setting. Thus, although the utility of physical methods for enhanced ocular drug delivery remains challenging, they are promising techniques that may have great impact on the clinical treatment of ocular diseases in the future.

Acknowledgements

The authors would like to thank the Health Research Council of New Zealand [14/018] and the Buchanan Charitable Foundation for their financial support.

References

[1] D. Pascolini, S.P. Mariotti, Global estimates of visual impairment: 2010, Br. J. Ophthalmol., 96 (2012) 614-618.

[2] A. Gordois, H. Cutler, L. Pezzullo, K. Gordon, A. Cruess, S. Winyard, W. Hamilton, K. Chua, An estimation of the worldwide economic and health burden of visual impairment, Glob. Public Health, 7 (2012) 465-481.

[3] R. Gaudana, H.K. Ananthula, A. Parenky, A.K. Mitra, Ocular drug delivery, AAPS J., 12 (2010) 348-360.

[4] K.C. Liu, C.R. Green, R.G. Alany, I.D. Rupenthal, Synergistic effect of chemical penetration enhancer and iontophoresis on transappendageal transport of oligodeoxynucleotides, Int. J. Pharm., 441 (2013) 687-692.

[5] P. Malik, R.S. Kadam, N.P. Cheruvu, U.B. Kompella, Hydrophilic prodrug approach for reduced pigment binding and enhanced transscleral retinal delivery of celecoxib, Mol. Pharm., 9 (2012) 605-614.

[6] L.N. Johnson, S.M. Cashman, R. Kumar-Singh, Cell-penetrating peptide for enhanced delivery of nucleic acids and drugs to ocular tissues including retina and cornea, Mol. Ther., 16 (2008) 107-114.

[7] Y. Dong, P. Dong, D. Huang, L. Mei, Y. Xia, Z. Wang, X. Pan, G. Li, C. Wu, Fabrication and characterization of silk fibroin-coated liposomes for ocular drug delivery, Eur. J. Pharm. Biopharm., 91 (2015) 82-90.

[8] R.T. Addo, K.G. Yeboah, R.C. Siwale, A. Siddig, A. Jones, R.V. Ubale, J. Akande, H. Nettey, N.J. Patel, E. Addo, M.J. D'Souza, Formulation and characterization of atropine sulfate in albumin-chitosan microparticles for *in vivo* ocular drug delivery, J. Pharm. Sci., 104 (2015) 1677-1690.

[9] E. Tratta, S. Pescina, C. Padula, P. Santi, S. Nicoli, In vitro permeability of a model protein across ocular tissues and effect of iontophoresis on the transscleral delivery, Eur. J. Pharm. Biopharm., 88 (2014) 116-122.

[10] W.L. Suen, H.S. Wong, Y. Yu, L.C. Lau, A.C. Lo, Y. Chau, Ultrasound-mediated transscleral delivery of macromolecules to the posterior segment of rabbit eye *in vivo*, Invest. Ophthalmol. Vis. Sci., 54 (2013) 4358-4365.

[11] J. Jiang, H.S. Gill, D. Ghate, B.E. McCarey, S.R. Patel, H.F. Edelhauser, M.R. Prausnitz, Coated microneedles for drug delivery to the eye, Invest. Ophthalmol. Vis. Sci., 48 (2007) 4038-4043.

[12] K. Tomoda, A. Watanabe, K. Suzuki, T. Inagi, H. Terada, K. Makino, Enhanced transdermal permeability of estradiol using combination of PLGA nanoparticles system and iontophoresis, Colloid Surf. B., 97 (2012) 84-89.

[13] M.J. Doughty, M.L. Zaman, Human corneal thickness and its impact on intraocular pressure measures: A review and meta-analysis approach, Surv. Ophthalmol., 44 (2000) 367-408.

[14] D.M. Maurice, S. Mishima, Ocular pharmacokinetics, in: Pharmacol. Eye, 1984, pp. 19-116.

[15] A. Edwards, M.R. Prausnitz, Predicted permeability of the cornea to topical drugs, Pharm. Res., 18 (2001) 1497-1508.

[16] H.S. Huang, R.D. Schoenwald, J.L. Lach, Corneal penetration behavior of beta-blocking agents II: Assessment of barrier contributions, J. Pharm. Sci., 72 (1983) 1272-1279.

[17] J.H. Liaw, Y.Y. Rojanasakul, J.R. Robinson, The effect of drug charge type and charge-density on corneal transport, Int. J. Pharm., 88 (1992) 111-124.

[18] Y.Y. Rojanasakul, J.R. Robinson, Transport mechanisms of the cornea-characterization of barrier permselectivity, Int. J. Pharm., 55 (1989) 237-246.

[19] N.J. Van Haeringen, E. Glasius, Lysosomal hydrolases in tears and the lacrimal gland: effect of acetylsalicylic acid on the release from the lacrimal gland, Invest. Ophthalmol. Vis. Sci., 19 (1980) 826-829.

[20] P.M. Hughes, O. Olejnik, J.E. Chang-Lin, C.G. Wilson, Topical and systemic drug delivery to the posterior segments, Adv. Drug Deliv. Rev., 57 (2005) 2010-2032.

[21] J. Pe'er, Conjunctival and corneal tumors: examination techniques, in: Clin. Ophthalmic. Oncology, Springer, 2014, pp. 139-142.

[22] M.A. Watsky, M.M. Jablonski, H.F. Edelhauser, Comparison of conjunctival and corneal surface areas in rabbit and human, Curr. Eye Res., 7 (1988) 483-486.

[23] K.M. Hamalainen, K. Kananen, S. Auriola, K. Kontturi, A. Urtti, Characterization of paracellular and aqueous penetration routes in cornea, conjunctiva, and sclera, Invest. Ophthalmol. Vis. Sci., 38 (1997) 627-634.

[24] A.J. Huang, S.C. Tseng, K.R. Kenyon, Paracellular permeability of corneal and conjunctival epithelia, Invest. Ophthalmol. Vis. Sci., 30 (1989) 684-689.

[25] T.F. Freddo, Shifting the paradigm of the blood-aqueous barrier, Exp. Eye Res., 73 (2001) 581-592.

[26] J. Barar, A.R. Javadzadeh, Y. Omidi, Ocular novel drug delivery: Impacts of membranes and barriers, Expert Opin. Drug Deliv., 5 (2008) 567-581.

[27] T.W. Olsen, S.Y. Aaberg, D.H. Geroski, H.F. Edelhauser, Human sclera: Thickness and surface area, Am. J. Ophthalmol., 125 (1998) 237-241.

[28] L.P.J. Cruysberg, R.M.M.A. Nuijts, D.H. Geroski, L.H. Koole, F. Hendrikse, H.F. Edelhauser, In vitro human scleral permeability of fluorescein, dexamethasone-fluorescein, methotrexate-fluorescein and rhodamine 6G and the use of a coated coil as a new drug delivery system, J. Ocul. Pharmacol. Th., 18 (2002) 559-569.

[29] J. Ambati, A.P. Adamis, Transscleral drug delivery to the retina and choroid, Prog. Retin. Eye Res., 21 (2002) 145-151.

[30] O.A. Boubriak, J.P. Urban, S. Akhtar, K.M. Meek, A.J. Bron, The effect of hydration and matrix composition on solute diffusion in rabbit sclera, Exp. Eye Res., 71 (2000) 503-514.

[31] J. Ambati, C.S. Canakis, J.W. Miller, E.S. Gragoudas, A. Edwards, D.J. Weissgold, I. Kim, F.C. Delori, A.P. Adamis, Diffusion of high molecular weight compounds through sclera, Invest. Ophthalmol. Vis. Sci., 41 (2000) 1181-1185.

[32] D.M. Maurice, J. Polgar, Diffusion across the sclera, Exp. Eye Res., 25 (1977) 577-582.

[33] S. Pescina, P. Govoni, M. Antopolsky, L. Murtomaki, C. Padula, P. Santi, S. Nicoli, Permeation of proteins, oligonucleotide and dextrans across ocular tissues: Experimental studies and a literature update, J. Pharm. Sci., 104 (2015) 2190-2202.

[34] A.A. Hussain, C. Starita, A. Hodgetts, J. Marshall, Macromolecular diffusion characteristics of ageing human Bruch's membrane: Implications for age-related macular degeneration (AMD), Exp. Eye Res., 90 (2010) 703-710.

[35] N.P. Cheruvu, U.B. Kompella, Bovine and porcine transscleral solute transport: Influence of lipophilicity and the Choroid-Bruch's layer, Invest. Ophthalmol. Vis. Sci., 47 (2006) 4513-4522.

[36] N.P. Cheruvu, A.C. Amrite, U.B. Kompella, Effect of eye pigmentation on transscleral drug delivery, Invest. Ophthalmol. Vis. Sci., 49 (2008) 333-341.

[37] J. Candiello, M. Balasubramani, E.M. Schreiber, G.J. Cole, U. Mayer, W. Halfter, H. Lin, Biomechanical properties of native basement membranes, FEBS J., 274 (2007) 2897-2908.

[38] M. Kamei, K. Misono, H. Lewis, A study of the ability of tissue plasminogen activator to diffuse into the subretinal space after intravitreal injection in rabbits, Am. J. Ophthalmol., 128 (1999) 739-746.

[39] T.L. Jackson, R.J. Antcliff, J. Hillenkamp, J. Marshall, Human retinal molecular weight exclusion limit and estimate of species variation, Invest. Ophthalmol. Vis. Sci., 44 (2003) 2141-2146.

[40] M.F. Marmor, A. Negi, D.M. Maurice, Kinetics of macromolecules injected into the subretinal space, Exp. Eye Res., 40 (1985) 687-696.

[41] E.A. Runkle, D.A. Antonetti, The blood-retinal barrier: structure and functional significance, in: The Blood-Brain and Other Neural Barriers, Springer, 2011, pp. 133-148.

[42] H.P. Hammes, J. Lin, O. Renner, M. Shani, A. Lundqvist, C. Betsholtz, M. Brownlee, U. Deutsch, Pericytes and the pathogenesis of diabetic retinopathy, Diabetes, 51 (2002) 3107-3012.

[43] R. Motiejunaite, A. Kazlauskas, Pericytes and ocular diseases, Exp. Eye Res., 86 (2008) 171-177.

[44] V. Kansara, A.K. Mitra, Evaluation of an *ex vivo* model implication for carrier-mediated retinal drug delivery, Curr. Eye Res., 31 (2006) 415-426.

[45] H. Sarin, Physiologic upper limits of pore size of different blood capillary types and another perspective on the dual pore theory of microvascular permeability, J. Angiogenes. Res., 2 (2010) 14.

[46] L. Pitkanen, V.P. Ranta, H. Moilanen, A. Urtti, Permeability of retinal pigment epithelium: Effects of permeant molecular weight and lipophilicity, Invest. Ophthalmol. Vis. Sci., 46 (2005) 641-646.

[47] M.R. Prausnitz, J.S. Noonan, Permeability of cornea, sclera, and conjunctiva: A literature analysis for drug delivery to the eye, J. Pharm. Sci., 87 (1998) 1479-1488.

[48] G. Grabner, G. Zehetbauer, H. Bettelheim, C. Honigsmann, W. Dorda, The blood-aqueous barrier and its permeability for proteins of different molecular weight, Graefes Arch. Clin. Exp. Ophthalmol., 207 (1978) 137-148.

[49] A. Urtti, Challenges and obstacles of ocular pharmacokinetics and drug delivery, Adv. Drug Deliv. Rev., 58 (2006) 1131-1145.

[50] S.H. Kim, R.J. Lutz, N.S. Wang, M.R. Robinson, Transport barriers in transscleral drug delivery for retinal diseases, Ophthalmic. Res., 39 (2006) 244-254.

[51] A.A. Hussain, L. Rowe, J. Marshall, Age-related alterations in the diffusional transport of amino acids across the human Bruch's-choroid complex, J. Opt. Soc. Am., 19 (2002) 166-172.

[52] D.B. Freilich, P.F. Lee, H.M. Freeman, Experimental retinal detachment, Arch. Ophthalmol., 76 (1966) 432-436.

[53] Y.N. Kalia, A. Naik, J. Garrison, R.H. Guy, Iontophoretic drug delivery, Adv. Drug Deliv. Rev., 56 (2004) 619-658.

[54] Y. Wang, R. Thakur, Q. Fan, B. Michniak, Transdermal iontophoresis: combination strategies to improve transdermal iontophoretic drug delivery, Eur. J. Pharm. Biopharm., 60 (2005) 179-191.

[55] M.B. Delgado-Charro, Iontophoretic drug delivery across the nail, Expert Opin. Drug Deliv., 9 (2012) 91-103.

[56] E. Eljarrat-Binstock, A.J. Domb, Iontophoresis: A non-invasive ocular drug delivery, J. Control. Release, 110 (2006) 479-489.

[57] R. Wirtz, Die Ionentherapie in der Augenheilkunde, Klein. Monatsbl. Augenheilkd., 46 (1908) 543-579.

[58] B. M., Transscleral iontophoresis of cefazolin, cicarcillin, and gentamicin in the rabbit, Ophthalmology, 93 (1986) 133-139.

[59] P. Chopra, J. Hao, S.K. Li, Iontophoretic transport of charged macromolecules across human sclera, Int. J. Pharm., 388 (2010) 107-113.

[60] J.G. Souza, K. Dias, S.A. Silva, L.C. de Rezende, E.M. Rocha, F.S. Emery, R.F. Lopez, Transcorneal iontophoresis of dendrimers: PAMAM corneal penetration and dexamethasone delivery, J. Control. Release, 200 (2015) 115-124.

[61] P. Chopra, J. Hao, S.K. Li, Sustained release micellar carrier systems for iontophoretic transport of dexamethasone across human sclera, J. Control. Release, 160 (2012) 96-104.

[62] R.H. Guy, Y.N. Kalia, M.B. Delgado-Charro, V. Merino, A. Lopez, D. Marro, Iontophoresis: Electrorepulsion and electroosmosis, J. Control. Release, 64 (2000) 129-132.

[63] D. Marro, Y.N. Kalia, M.B. Delgado-Charro, R.H. Guy, Contributions of electromigration and electroosmosis to iontophoretic drug delivery, Pharm. Res., 18 (2001) 1701-1708.

[64] G.B. Kasting, Theoretical-models for iontophoretic delivery, Adv. Drug Deliv. Rev., 9 (1992) 177-199.

[65] S. Nicoli, G. Ferrari, M. Quarta, C. Macaluso, P. Santi, *In vitro* transscleral iontophoresis of high molecular weight neutral compounds, Eur. J. Pharm. Sci., 36 (2009) 486-492.

[66] L. Murtomaki, T. Vainikka, S. Pescina, S. Nicoli, Drug adsorption on bovine and porcine sclera studied with streaming potential, J. Pharm. Sci., 102 (2013) 2264-2272.

[67] S. Pescina, D. Martini, P. Santi, C. Padula, L. Murtomaki, S. Nicoli, *In vitro* trans-scleral iontophoresis of methylprednisolone hemisuccinate with short application time and high drug concentration, Int. J. Pharm., 451 (2013) 12-17.

[68] A.E. Cohen, C. Assang, M.A. Patane, S. From, M. Korenfeld, I. Avion Study, Evaluation of dexamethasone phosphate delivered by ocular iontophoresis for treating noninfectious anterior uveitis, Ophthalmology, 119 (2012) 66-73.

[69] Eyegate Pharmaceuticals, Inc., Safety and efficacy study of iontophoretic dexamethasone phosphate ophthalmic solution to treat non-infectious anterior segment uveitis, in, ClinicalTrials.gov, National Library of Medicine (USA), Bethesda (MD), 2012, www.clinicaltrials.gov/ct2/show/NCT01505088 (cited 12 August 2016).

[70] M.A. Patane, A. Cohen, S. From, G. Torkildsen, D. Welch, G.W. Ousler, 3rd, Ocular iontophoresis of EGP-437 (dexamethasone phosphate) in dry eye patients: Results of a randomized clinical trial, Clin. Ophthalmol., 5 (2011) 633-643.

[71] Eyegate Pharmaceuticals, Inc., Safety and efficacy study of EGP-437 (dexamethasone phosphate formulated for ccular iontophoresis) to treat dry eye, in, ClinicalTrials.gov, National Library of Medicine (USA), Bethesda (MD), 2010, www.clinicaltrials.gov/ct2/show/NCT01129856 (cited 12 August 2016).

[72] Eyegate Pharmaceuticals, Inc., Open-label, multli-center, phase 1b/2a clinical trial designed to evaluate the safety and efficacy of iontophoretic dexamethasone phosphate ophthalmic solution in patients with macular edema, in, ClinicalTrials.gov, National Library of Medicine (USA), Bethesda (MD), 2015, www.clinicaltrials.gov/ct2/show/NCT02485249 (cited 12 August 2016).

[73] http://www.eyegatepharma.com/technology/pipeline (cited 12 August 2016).

[74] Eyegate Pharmaceuticals, Inc., Safety and efficacy study of iontophoretic dexamethasone phosphate ophthalmic solution in patients undergoing cataract surgery with implantation of a posterior chamber intraocular lens, in, ClinicalTrials.gov, National Library of Medicine (USA), Bethesda (MD), 2012, www.clinicaltrials.gov/ct2/show/NCT01602068 (cited 12 August 2016).

[75] Y. Zhang, Y. Chen, X. Yu, Y. Qi, D. Huang, M. Yang, X. Yu, Y. Hu, Z. Li, An ocular iontophoretic device using PEDOT electrode for local drug delivery, Sens. Actuators B-Chem., (2016).

[76] Y. Zhang, Y. Chen, X. Yu, Y. Qi, Y. Chen, Y. Liu, Y. Hu, Z. Li, A flexible device for ocular iontophoretic drug delivery, Biomicrofluidics, 10 (2016) 011911.

[77] E. Eljarrat-Binstock, A.J. Domb, F. Orucov, A. Dagan, J. Frucht-Pery, J. Pe'er, *In vitro* and *in vivo* evaluation of carboplatin delivery to the eye using hydrogel-iontophoresis, Curr. Eye Res., 33 (2008) 269-275.

[78] E. Eljarrat-Binstock, F. Raiskup, D. Stepensky, A.J. Domb, J. Frucht-Pery, Delivery of gentamicin to the rabbit eye by drug-loaded hydrogel iontophoresis, Invest. Ophthalmol. Vis. Sci., 45 (2004) 2543-2548.

[79] E. Eljarrat-Binstock, F. Raiskup, J. Frucht-Pery, A.J. Domb, Transcorneal and transscleral iontophoresis of dexamethasone phosphate using drug loaded hydrogel, J. Control. Release, 106 (2005) 386-390.

[80] E. Eljarrat-Binstock, F. Orucov, J. Frucht-Pery, J. Pe'er, A.J. Domb, Methylprednisolone delivery to the back of the eye using hydrogel iontophoresis, J. Ocul. Pharmacol. Ther., 24 (2008) 344-350.

[81] E. Eljarrat-Binstock, F. Orucov, Y. Aldouby, J. Frucht-Pery, A.J. Domb, Charged nanoparticles delivery to the eye using hydrogel iontophoresis, J. Control. Release, 126 (2008) 156-161.

[82] G.A. Fisher, T.M. Parkinson, M.A. Szlek, OcuPhor™-The future of ocular drug delivery, Drug Dev. Deliv., 2 (2002).

[83] T.M. Parkinson, E. Ferguson, S. Febbraro, A. Bakhtyari, M. King, M. Mundasad, Tolerance of ocular iontophoresis in healthy volunteers, J. Ocul. Pharmacol. Ther., 19 (2003) 145-151.

[84] D.L. Vollmer, M.A. Szlek, K. Kolb, L.B. Lloyd, T.M. Parkinson, *In vivo* transscleral iontophoresis of amikacin to rabbit eyes, J. Ocul. Pharmacol. Ther., 18 (2002) 549-558.

[85] M.S. Hastings, S.K. Li, D.J. Miller, P.S. Bernstein, D. Mufson, Visulex: Advancing iontophoresis for effective noninvasive back-to-the-eye therapeutics, Drug Deliv. Tech., 4 (2004) 53-57.

[86] http://www.aciont.com/product_pipeline/ (cited 12 August 2016).

[87] Aciont Inc., Safety and efficacy study of DSP-Visulex for the treatment of anterior uveitis, in, ClinicalTrials.gov, National Library of Medicine (USA), Bethesda (MD), 2014, www.clinicaltrials.gov/ct2/show/NCT02309385 (cited 12 August 2016).

[88] J. Higuchi, K. Papangkorn, S. Molokhia, D. Mix, C. Butler, P. Karra, B. Brar, S.K. Li, W.I. Higuchi, Transscleral iontophoretic delivery of a macromolecule into the rabbit eye, Invest. Ophthalmol. Vis. Sci., 53 (2012) 464.

[89] S.A. Molokhia, K. Papangkorn, D. Mix, C. Butler, P. Karra, J. Higuchi, B. Brar, S.K. Li, W.I. Higuchi, Transscleral iontophoretic delivery of Avastin® *in vivo*: Drug distribution and safety aspects, Invest. Ophthalmol. Vis. Sci., 53 (2012) 491.

[90] S.R. Kiran Vaka, S.M. Sammeta, L.B. Day, S.N. Murthy, Transcorneal iontophoresis for delivery of ciprofloxacin hydrochloride, Curr. Eye Res., 33 (2008) 661-667.

[91] J. Frucht-Pery, F. Raiskup, H. Mechoulam, M. Shapiro, E. Eljarrat-Binstock, A. Domb, Iontophoretic treatment of experimental pseudomonas keratitis in rabbit eyes using gentamicin-loaded hydrogels, Cornea, 25 (2006) 1182-1186.

[92] J. Frucht-Pery, H. Mechoulam, C.S. Siganos, P. Ever-Hadani, M. Shapiro, A. Domb, Iontophoresis-gentamicin delivery into the rabbit cornea using a hydrogel delivery probe, Exp. Eye Res., 78 (2004) 745-749.

[93] D. Monti, L. Saccomani, P. Chetoni, S. Burgalassi, M.F. Saettone, Effect of iontophoresis on transcorneal permeation '*in vitro*'of two β-blocking agents, and on corneal hydration, Int. J. Pharm., 250 (2003) 423-429.

[94] T. Asahara, K. Shinomiya, T. Naito, H. Shiota, Induction of gene into the rabbit eye by iontophoresis: preliminary report, Jpn. J. Ophthalmol., 45 (2001) 31-39.

[95] J. Hao, S.K. Li, C.Y. Liu, W.W. Kao, Electrically assisted delivery of macromolecules into the corneal epithelium, Exp. Eye Res., 89 (2009) 934-941.

[96] H. Sekijima, J. Ehara, Y. Hanabata, T. Suzuki, S. Kimura, V.H. Lee, Y. Morimoto, H. Ueda, Characterization of ocular iontophoretic drug transport of ionic and non-ionic compounds in isolated rabbit cornea and conjunctiva, Biol. Pharm. Bull., 39 (2016) 959-968.

[97] M. Berdugo, F. Valamanesh, C. Andrieu, C. Klein, D. Benezra, Y. Courtois, F. Behar-Cohen, Delivery of antisense oligonucleotide to the cornea by iontophoresis, Antisense Nucleic Acid Drug Dev., 13 (2003) 107-114.

[98] M. Voigt, Y. de Kozak, M. Halhal, Y. Courtois, F. Behar-Cohen, Down-regulation of NOSII gene expression by iontophoresis of anti-sense oligonucleotide in endotoxin-induced uveitis, Biochem. Biophys. Res. Commun., 295 (2002) 336-341.

[99] E. Eljarrat-Binstock, F. Raiskup, J. Frucht-Pery, A.J. Domb, Hydrogel probe for iontophoresis drug delivery to the eye, J. Biomater. Sci. Polym. Ed., 15 (2004) 397-413.

[100] B. Hayden, M.E. Jockovich, T.G. Murray, M.T. Kralinger, M. Voigt, E. Hernandez, W. Feuer, J.M. Parel, Iontophoretic delivery of carboplatin in a murine model of retinoblastoma, Invest. Ophthalmol. Vis. Sci., 47 (2006) 3717-3721.

[101] S. Gungor, M.B. Delgado-Charro, B. Ruiz-Perez, W. Schubert, P. Isom, P. Moslemy, M.A. Patane, R.H. Guy, Trans-scleral iontophoretic delivery of low molecular weight therapeutics, J. Control. Release, 147 (2010) 225-231.

[102] S. Pescina, G. Ferrari, P. Govoni, C. Macaluso, C. Padula, P. Santi, S. Nicoli, *In-vitro* permeation of bevacizumab through human sclera: Effect of iontophoresis application, J. Pharm. Pharmacol., 62 (2010) 1189-1194.

[103] S. Pescina, M. Antopolsky, P. Santi, S. Nicoli, L. Murtomaki, Effect of iontophoresis on the *in vitro* trans-scleral transport of three single stranded oligonucleotides, Eur. J. Pharm. Sci., 49 (2013) 142-147.

[104] E.H. Souied, S.N. Reid, N.I. Piri, L.E. Lerner, S. Nusinowitz, D.B. Farber, Non-invasive gene transfer by iontophoresis for therapy of an inherited retinal degeneration, Exp. Eye Res., 87 (2008) 168-175.

[105] J. Goodchild, Therapeutic oligonucleotides, in: Therapeutic Oligonucleotides, Springer, 2011, pp. 1-15.

[106] M.T. Kralinger, M. Voigt, G. Kieselbach, D. Hamasaki, B. Hayden, J.M. Parel, Ocular delivery of acetylsalicylic acid by repetitive coulomb-controlled iontophoresis, Ophthalmic. Res., 35 (2002) 102-110.

[107] E. Eljarrat-Binstock, A.J. Domb, F. Orucov, J. Frucht-Pery, J. Pe'er, Methotrexate delivery to the eye using transscleral hydrogel iontophoresis, Curr. Eye Res., 32 (2007) 639-646.

[108] S.A. Molokhia, E.K. Jeong, W.I. Higuchi, S.K. Li, Transscleral iontophoretic and intravitreal delivery of a macromolecule: study of ocular distribution *in vivo* and postmortem with MRI, Exp. Eye Res., 88 (2009) 418-425.

[109] S. Pescina, C. Padula, P. Santi, S. Nicoli, Effect of formulation factors on the trans-scleral iontophoretic and post-iontophoretic transports of a 40kDa dextran *in vitro*, Eur. J. Pharm. Sci., 42 (2011) 503-508.

[110] P. Chopra, J. Hao, S.K. Li, Influence of drug lipophilicity on drug release from sclera after iontophoretic delivery of mixed micellar carrier system to human sclera, J. Pharm. Sci., 102 (2013) 480-488.

[111] Y. Oshima, T. Sakamoto, I. Yamanaka, T. Nishi, T. Ishibashi, H. Inomata, Targeted gene transfer to corneal endothelium *in vivo* by electric pulse, Gene Ther., 5 (1998) 1347-1354.

[112] A.K. Banga, S. Bose, T.K. Ghosh, Iontophoresis and electroporation: Comparisons and contrasts, Int. J. Pharm., 179 (1999) 1-19.

[113] E. Neumann, M. Schaeferridder, Y. Wang, P.H. Hofschneider, Gene-transfer into mouse lyoma cells by electroporation in high electric-fields, EMBO J., 1 (1982) 841-845.

[114] J. Gehl, L.M. Mir, Determination of optimal parameters for *in vivo* gene transfer by electroporation, using a rapid *in vivo* test for cell permeabilization, Biochem. Biophys. Res. Commun., 261 (1999) 377-380.

[115] Y.A. Chizmadzhev, A.V. Indenbom, P.I. Kuzmin, S.V. Galichenko, J.C. Weaver, R.O. Potts, Electrical properties of skin at moderate voltages: Contribution of appendageal macropores, Biophys. J., 74 (1998) 843-856.

[116] F. Apollonio, M. Liberti, P. Marracino, L. Mir, Electroporation mechanism: Review of molecular models based on computer simulation, in: Antennas and Propagation (EUCAP), 2012 6th European Conference, IEEE, 2012, pp. 356-358.

[117] D.P. Tieleman, The molecular basis of electroporation, BMC Biochem., 5 (2004) 10.

[118] Q. Hu, R.P. Joshi, K.H. Schoenbach, Simulations of nanopore formation and phosphatidylserine externalization in lipid membranes subjected to a high-intensity, ultrashort electric pulse, Phys. Rev., 72 (2005) 031902.

[119] M. Tarek, Membrane electroporation: A molecular dynamics simulation, Biophys. J., 88 (2005) 4045-4053.

[120] J. Teissie, M. Golzio, M.P. Rols, Mechanisms of cell membrane electropermeabilization: A minireview of our present (lack of?) knowledge, Biochem. Biophys. Acta., 1724 (2005) 270-280.

[121] C. Chen, S.W. Smye, M.P. Robinson, J.A. Evans, Membrane electroporation theories: A review, Med. Biol. Eng. Comput., 44 (2006) 5-14.

[122] I. Zampaglione, M. Arcuri, M. Cappelletti, G. Ciliberto, G. Perretta, A. Nicosia, N. La Monica, E. Fattori, *In vivo* DNA gene electro-transfer: A systematic analysis of different electrical parameters, J. Gene Med., 7 (2005) 1475-1481.

[123] D.J. Wells, Gene therapy progress and prospects: Electroporation and other physical methods, Gene Ther., 11 (2004) 1363-1369.

[124] S. Mehier-Humbert, R.H. Guy, Physical methods for gene transfer: Improving the kinetics of gene delivery into cells, Adv. Drug Deliv. Rev., 57 (2005) 733-753.

[125] K. Blair‐Parks, B.C. Weston, D.A. Dean, High‐level gene transfer to the cornea using electroporation, J. Gene Med., 4 (2002) 92-100.

[126] E. Touchard, M. Berdugo, P. Bigey, M. El Sanharawi, M. Savoldelli, M.C. Naud, J.C. Jeanny, F. Behar-Cohen, Suprachoroidal electrotransfer: A nonviral gene delivery method to transfect the choroid and the retina without detaching the retina, Mol. Ther., 20 (2012) 1559-1570.

[127] V. Zderic, J.I. Clark, S. Vaezy, Drug delivery into the eye with the use of ultrasound, J. Ultras. Med., 23 (2004) 1349-1359.

[128] B.E. Polat, D. Hart, R. Langer, D. Blankschtein, Ultrasound-mediated transdermal drug delivery: Mechanisms, scope, and emerging trends, J. Control. Release, 152 (2011) 330-348.

[129] G.H. Mundt, Jr., W.F. Hughes, Jr., Ultrasonics in ocular diagnosis, Am. J. Ophthalmol., 41 (1956) 488-498.

[130] F. Aptel, C. Lafon, Treatment of glaucoma with high intensity focused ultrasound, Int. J. Hyperther., 31 (2015) 292-301.

[131] M. Nabili, H. Patel, S.P. Mahesh, J. Liu, C. Geist, V. Zderic, Ultrasound-enhanced delivery of antibiotics and anti-inflammatory drugs into the eye, Ultras. Med. Biol., 39 (2013) 638-646.

[132] T. Yamashita, S. Sonoda, R. Suzuki, N. Arimura, K. Tachibana, K. Maruyama, T. Sakamoto, A novel bubble liposome and ultrasound-mediated gene transfer to ocular surface: RC-1 cells *in vitro* and conjunctiva *in vivo*, Exp. Eye Res., 85 (2007) 741-748.

[133] A.C. Cheung, Y. Yu, D. Tay, H.S. Wong, R. Ellis-Behnke, Y. Chau, Ultrasound-enhanced intrascleral delivery of protein, Int. J. Pharm., 401 (2010) 16-24.

[134] M. Lafond, F. Aptel, J.L. Mestas, C. Lafon, Ultrasound-mediated ocular delivery of therapeutic agents: a review, Expert Opin. Drug Deliv., (2016) 1-12.

[135] S. Mitragotri, D.A. Edwards, D. Blankschtein, R. Langer, A mechanistic study of ultrasonically-enhanced transdermal drug delivery, J. Pharm. Sci., 84 (1995) 697-706.

[136] D.L. Miller, A review of the ultrasonic bioeffects of microsonation, gas-body activation, and related cavitation-like phenomena, Ultras. Med. Biol., 13 (1987) 443-470.

[137] T. Leighton, The acoustic bubble, Academic Press, 2012.

[138] W.L. Suen, J. Jiang, H.S. Wong, J. Qu, Y. Chau, Examination of effects of low-frequency ultrasound on scleral permeability and collagen network, Ultras. Med. Biol., 42 (2016) 2650-2661.

[139] I. Lentacker, S.C. De Smedt, N.N. Sanders, Drug loaded microbubble design for ultrasound triggered delivery, Soft Matter., 5 (2009) 2161-2170.

[140] V.F. Humphrey, Ultrasound and matter-Physical interactions, Prog. Biophys. Mol. Bio., 93 (2007) 195-211.

[141] A. Razavi, D. Clement, R.A. Fowler, A. Birer, F. Chavrier, J.L. Mestas, F. Romano, J.Y. Chapelon, A. Begle, C. Lafon, Contribution of inertial cavitation in the enhancement of *in vitro* transscleral drug delivery, Ultras. Med. Biol., 40 (2014) 1216-1227.

[142] V. Zderic, S. Vaezy, R.W. Martin, J.I. Clark, Ocular drug delivery using 20-kHz ultrasound, Ultras. Med. Biol., 28 (2002) 823-829.

[143] L. Kowalczuk, M. Boudinet, M. El Sanharawi, E. Touchard, M.C. Naud, A. Saied, J.C. Jeanny, F. Behar-Cohen, P. Laugier, *In vivo* gene transfer into the ocular ciliary muscle mediated by ultrasound and microbubbles, Ultras. Med. Biol., 37 (2011) 1814-1827.

[144] S.B. Barnett, G.R. Ter Haar, M.C. Ziskin, H.D. Rott, F.A. Duck, K. Maeda, International recommendations and guidelines for the safe use of diagnostic ultrasound in medicine, Ultras. Med. Biol., 26 (2000) 355-366.

[145] M. Nabili, C. Geist, V. Zderic, Thermal safety of ultrasound-enhanced ocular drug delivery: A modeling study, Med. Phys., 42 (2015) 5604-5615.

[146] E.F.o.S.f.U.i.M.a. Biology, European Committee for Medical Ultrasound Safety Bylaw, in, Newsletter 12, 1998.

[147] X.H. Wang, H.D. Liang, B.W. Dong, Q.L. Lu, M.J.K. Blomley, Gene transfer with microbubble ultrasound and plasmid DNA into skeletal muscle of mice: comparison between commercially available microbubble contrast agents 1, Radiology, 237 (2005) 224-229.

[148] S. Sonoda, K. Tachibana, E. Uchino, A. Okubo, M. Yamamoto, K. Sakoda, T. Hisatomi, K.H. Sonoda, Y. Negishi, Y. Izumi, S. Takao, T. Sakamoto, Gene transfer to corneal epithelium and keratocytes mediated by ultrasound with microbubbles, Invest. Ophthalmol. Vis. Sci., 47 (2006) 558-564.

[149] D. Huang, L.L. Wang, Y.X. Dong, X. Pan, G. Li, C.B. Wu, A novel technology using transscleral ultrasound to deliver protein loaded nanoparticles, Eur. J. Pharm. Biopharm., 88 (2014) 104-115.

[150] D. Huang, Y.S. Chen, I.D. Rupenthal, Ultrasound-mediated nanoparticle delivery across ex vivo bovine retina after intravitreal injection, Eur. J. Pharm. Biopharm., 119 (2017) 125-136.

[151] F. Aptel, T. Charrel, C. Lafon, F. Romano, J.Y. Chapelon, E. Blumen-Ohana, J.P. Nordmann, P. Denis, Miniaturized high-intensity focused ultrasound device in patients with glaucoma: A clinical pilot study, Invest. Ophthalmol. Vis. Sci., 52 (2011) 8747-8753.

[152] P. Denis, F. Aptel, J.F. Rouland, J.P. Nordmann, Y. Lachkar, J.P. Renard, E. Sellem, C. Baudouin, B. Alain, Cyclocoagulation of the ciliary bodies by high intensity focused ultrasound (HIFU): a 12-month multicenter study, Invest. Ophthalmol. Vis. Sci., (2015) IOVS-14-14973.

[153] F. Aptel, P. Denis, J.F. Rouland, J.P. Renard, A. Bron, Multicenter clinical trial of high‐intensity focused ultrasound treatment in glaucoma patients without previous filtering surgery, Acta Ophthalmol., 94 (2016) e268-e277.

[154] S.K. Murugappan, Y. Zhou, Transsclera Drug Delivery by Pulsed High-Intensity Focused Ultrasound (HIFU): An Ex Vivo Study, Curr. Eye Res., 40 (2015) 1172-1180.

[155] S.S. Thakur, N.L. Barnett, M.J. Donaldson, H.S. Parekh, Intravitreal drug delivery in retinal disease: Are we out of our depth?, Expert Opin. Drug Deliv., 11 (2014) 1575-1590.

[156] T.Y. Wang, K.E. Wilson, S. Machtaler, J.K. Willmann, Ultrasound and microbubble guided drug delivery: Mechanistic understanding and clinical implications, Curr. Pharm. Biotechno., 14 (2013) 743-752.

[157] L. Peeters, I. Lentacker, R.E. Vandenbroucke, B. Lucas, J. Demeester, N.N. Sanders, S.C. De Smedt, Can ultrasound solve the transport barrier of the neural retina?, Pharm. Res., 25 (2008) 2657-2665.

[158] H.L. Li, X.Z. Zheng, H.P. Wang, F. Li, Y. Wu, L.F. Du, Ultrasound-targeted microbubble destruction enhances AAV-mediated gene transfection in human RPE cells *in vitro* and rat retina *in vivo*, Gene Ther., 16 (2009) 1146-1153.

[159] S. Sonoda, K. Tachibana, T. Yamashita, M. Shirasawa, H. Terasaki, E. Uchino, R. Suzuki, K. Maruyama, T. Sakamoto, Selective gene transfer to the retina using intravitreal ultrasound irradiation, J. Ophthalmol., 2012 (2012) 1-5.

[160] J. Park, Y. Zhang, N. Vykhodtseva, J.D. Akula, N.J. McDannold, Targeted and reversible blood-retinal barrier disruption via focused ultrasound and microbubbles, PLoS One, 7 (2012) e42754.

[161] M. Nabili, A. Shenoy, S. Chawla, S. Mahesh, J. Liu, C. Geist, V. Zderic, Ultrasound-enhanced ocular delivery of dexamethasone sodium phosphate: an in vivo study, J. Ther. Ultras., 2 (2014) 6.

[162] Y. Chau, W.L.L. Suen, H.Y. Tse, H.S. Wong, Ultrasound-enhanced penetration through sclera depends on frequency of sonication and size of macromolecules, Eur. J. Pharm. Sci., 100 (2017) 273-279.

[163] R.F. Donnelly, T.R. Raj Singh, A.D. Woolfson, Microneedle-based drug delivery systems: microfabrication, drug delivery, and safety, Drug Deliv., 17 (2010) 187-207.

[164] Y.C. Kim, J.H. Park, M.R. Prausnitz, Microneedles for drug and vaccine delivery, Adv. Drug Deliv. Rev., 64 (2012) 1547-1568.

[165] O. Khandan, A. Famili, M.Y. Kahook, M.P. Rao, Titanium-based, fenestrated, in-plane microneedles for passive ocular drug delivery, in: Engineering in Medicine and Biology Society (EMBC), 2012 Annual International Conference of the IEEE, IEEE, 2012, pp. 6572-6575.

[166] O. Khandan, M.Y. Kahook, M.P. Rao, Fenestrated microneedles for ocular drug delivery, Sens. Actuator B-Chem., 223 (2016) 15-23.

[167] Y.C. Kim, H.E. Grossniklaus, H.F. Edelhauser, M.R. Prausnitz, Intrastromal delivery of bevacizumab using microneedles to treat corneal neovascularization, Invest. Ophthalmol. Vis. Sci., 55 (2014) 7376-7386.

[168] H.B. Song, K.J. Lee, I.H. Seo, J.Y. Lee, S.M. Lee, J.H. Kim, J.H. Kim, W. Ryu, Impact insertion of transfer-molded microneedle for localized and minimally invasive ocular drug delivery, J. Control. Release, 209 (2015) 272-279.

[169] J. Jiang, J.S. Moore, H.F. Edelhauser, M.R. Prausnitz, Intrascleral drug delivery to the eye using hollow microneedles, Pharm. Res., 26 (2009) 395-403.

[170] R.R. Thakur, S.J. Fallows, H.L. McMillan, R.F. Donnelly, D.S. Jones, Microneedle-mediated intrascleral delivery of in situ forming thermoresponsive implants for sustained ocular drug delivery, J. Pharm. Pharmacol., 66 (2014) 584-595.

[171] G. Mahadevan, H. Sheardown, P. Selvaganapathy, PDMS embedded microneedles as a controlled release system for the eye, J. Biomater. Appl., 28 (2013) 20-27.

[172] R.R. Thakur, I. Tekko, K. McAvoy, H. McMillan, D. Jones, R.F. Donnelly, Minimally invasive microneedles for ocular drug delivery, Expert Opin. Drug Deliv., (2016) 1-13.

[173] R.R. Thakur, I.A. Tekko, F. Al-Shammari, A.A. Ali, H. McCarthy, R.F. Donnelly, Rapidly dissolving polymeric microneedles for minimally invasive intraocular drug delivery, Drug Deliv. Transl. Res., 6 (2016) 800-815.

[174] N.K. Palakurthi, Z.M. Correa, J.J. Augsburger, R.K. Banerjee, Toxicity of a biodegradable microneedle implant loaded with methotrexate as a sustained release device in normal rabbit eye: A pilot study, J. Ocul. Pharmacol. Ther., 27 (2011) 151-156.

[175] U.D.J.P. Rai, S.A. Young, T.R. Thrimawithana, H. Abdelkader, A.W.G. Alani, B. Pierscionek, R.G. Alany, The suprachoroidal pathway: A new drug delivery route to the back of the eye, Drug Discov. Today, 20 (2015) 491-495.

[176] S.R. Patel, A.S.P. Lin, H.F. Edelhauser, M.R. Prausnitz, Suprachoroidal drug delivery to the back of the eye using hollow microneedles, Pharm. Res., 28 (2011) 166-176.

[177] B. Chiang, Y.C. Kim, H.F. Edelhauser, M.R. Prausnitz, Circumferential flow of particles in the suprachoroidal space is impeded by the posterior ciliary arteries, Exp. Eye Res., 145 (2016) 424-431.

[178] R.S. Kadam, J. Williams, P. Tyagi, H.F. Edelhauser, U.B. Kompella, Suprachoroidal delivery in a rabbit *ex vivo* eye model: Influence of drug properties, regional differences in delivery, and comparison with intravitreal and intracameral routes, Mol. Vis., 19 (2013) 1198-1210.

[179] S.R. Patel, D.E. Berezovsky, B.E. McCarey, V. Zarnitsyn, H.F. Edelhauser, M.R. Prausnitz, Targeted administration into the suprachoroidal space using a microneedle for drug delivery to the posterior segment of the eye, Invest. Ophthalmol. Vis. Sci., 53 (2012) 4433-4441.

[180] B. Chiang, Y.C. Kim, A.C. Doty, H.E. Grossniklaus, S.P. Schwendeman, M.R. Prausnitz, Sustained reduction of intraocular pressure by supraciliary delivery of brimonidine-loaded poly(lactic acid) microspheres for the treatment of glaucoma, J. Control. Release, 228 (2016) 48-57.

[181] Y.C. Kim, K.H. Oh, H.F. Edelhauser, M.R. Prausnitz, Formulation to target delivery to the ciliary body and choroid via the suprachoroidal space of the eye using microneedles, Eur. J. Pharm. Biopharm., 95 (2015) 398-406.

[182] B.C. Gilger, E.M. Abarca, J.H. Salmon, S. Patel, Treatment of acute posterior uveitis in a porcine model by injection of triamcinolone acetonide into the suprachoroidal space using microneedles, Invest. Ophthalmol. Vis. Sci., 54 (2013) 2483-2492.

[183] Clearside Biomedical, Inc., Suprachoroidal injection of triamcinolone acetonide in subjects with macular edema following non-infectious uveitis (DOGWOOD), in, ClinicalTrials.gov, National Library of Medicine (USA), Bethesda (MD), 2014, www.clinicaltrials.gov/ct2/show/NCT02255032 (cited 12 August 2016).

[184] Clearside Biomedical, Inc., Suprachoroidal injection of CLS-TA in subjects with macular edema associated with non-infectious uveitis (PEACHTREE), in, ClinicalTrials.gov, National Library of Medicine (USA), Bethesda (MD), 2015, www.clinicaltrials.gov/ct2/show/NCT02595398 (cited 12 August 2016).

[185] Clearside Biomedical, Inc., Suprachoroidal injection of triamcinolone acetonide with IVT aflibercept in subjects with macular edema following RVO (TANZANITE), in, ClinicalTrials.gov, National Library of Medicine (USA), Bethesda (MD), 2014, www.clinicaltrials.gov/ct2/show/NCT02303184 (cited 12 August 2016).

[186] Y.C. Kim, H.F. Edelhauser, M.R. Prausnitz, Targeted delivery of antiglaucoma drugs to the supraciliary space using microneedles, Invest. Ophthalmol. Vis. Sci., 55 (2014) 7387-7397.

[187] F.F. Behar-Cohen, A. El Aouni, S. Gautier, G. David, J. Davis, P. Chapon, J.M. Parel, Transscleral Coulomb-controlled iontophoresis of methylprednisolone into the rabbit eye: influence of duration of treatment, current intensity and drug concentration on ocular tissue and fluid levels, Exp. Eye Res., 74 (2002) 51-59.

[188] T. Gratieri, V. Santer, Y.N. Kalia, Basic principles and current status of transcorneal and transscleral iontophoresis, Expert Opin. Drug Deliv., (2016) 1-12.

[189] US FDA, Information for manufacturers seeking marketing clearance of diagnostic ultrasound systems and transducers, in, Center for Devices and Radiological Health, US Department of Health and Human Services, Food and Drug Administration, 1997.

[190] S.B. Barnett, F. Duck, M. Ziskin, WFUMB Symposium on Safety of Ultrasound in Medicine: conclusions and recommendations on biological effects and safety of ultrasound contrast agents, Ultras. Med. Biol., 33 (2007) 233-234.

[191] H. El Chehab, A. Le Corre, E. Agard, G. Ract-Madoux, O. Coste, C. Dot, Effect of topical pressure-lowering medication on prevention of intraocular pressure spikes after intravitreal injection, Eur. J. Ophthalmol., 23 (2013) 277-283.